Title: Overcoming immune evasion from post-translational modification of a mutant KRAS epitope to achieve TCR-T cell-mediated antitumor activity

Authors: Jihoon William Lee[1,2], Emily Y. Chen[1], Taylor Hu[1], Rachel Perret[1], Mary E. Chaffee[1], Tijana Martinov[1], Shwetha Mureli[1], Clara L. McCurdy[1], Lisa A. Jones[3], Philip R. Gafken[3], Pritha Chanana[4], Yapeng Su[1,5], Aude G. Chapuis[1,6], Philip Bradley[5], Thomas M. Schmitt[1†*], Philip D. Greenberg[1,6,7†*].

Affiliations:

[1] Program in Immunology, Division of Translational Science and Therapeutics, Fred Hutchinson Cancer Center, Seattle, WA, USA

[2] Medical Scientist Training Program, University of Washington, Seattle, WA, USA

[3] Proteomics and Metabolomics Shared Resource, Fred Hutchinson Cancer Center, Seattle, WA, USA

[4] Genomics and Bioinformatics Shared Resource, Fred Hutchinson Cancer Center, Seattle, WA, USA

[5] Herbold Computational Biology Program, Fred Hutchinson Cancer Center, Seattle, WA

[6] Department of Medicine, Division of Hematology and Oncology, University of Washington, Seattle, Washington, USA

[7] Department of Immunology, University of Washington, Seattle, WA

† Corresponding author(s): Philip Greenberg, MD, Thomas Schmitt, PhD

* Co-senior authors who contributed equally.

One-sentence summary: Tumor cell methylation of $KRAS_{G12V}$ epitope in HLA-A2 permits immune evasion, and new TCRs were generated to overcome this with engineered cell therapy.

Abstract

T cell receptor (TCR)-T cell immunotherapy, in which T cells are engineered to express a TCR targeting a tumor epitope, is a form of adoptive cell therapy (ACT) that has exhibited promise against various tumor types. Mutants of oncoprotein KRAS, particularly at glycine-12 (G12), are frequent drivers of tumorigenicity, making them attractive targets for TCR-T cell therapy. However, class I-restricted TCRs specifically targeting G12-mutant KRAS epitopes in the context of tumors expressing HLA-A2, the most common human HLA-A allele, have remained elusive despite evidence an epitope encompassing such mutations can bind HLA-A2 and induce T cell responses. We report post-translational modifications (PTMs) on this epitope may allow tumor cells to evade immunologic pressure from TCR-T cells. A lysine side chain-methylated $KRAS_{G12V}$ peptide, rather than the unmodified epitope, may be presented in HLA-A2 by tumor cells and impact TCR recognition. Using a novel computationally guided approach, we developed by mutagenesis TCRs that recognize this methylated peptide, enhancing tumor recognition and destruction. Additionally, we identified TCRs with similar functional activity in normal repertoires from primary T cells by stimulation with modified peptide, clonal expansion, and selection. Mechanistically, a gene knockout screen to identify mechanism(s) by which tumor cells methylate/demethylate this epitope unveiled SPT6 as a demethylating protein that could be targeted to improve effectiveness of these new TCRs. Our findings highlight the role of PTMs in immune evasion and suggest identifying and targeting such modifications should make effective ACTs available for a substantially greater range of tumors than the current therapeutic landscape.

Introduction

25 T cell receptors (TCRs) specific for a tumor-derived MHC class I epitope can be transduced into
26 patient T cells for adoptive cell therapy (ACT) to achieve promising antitumor effects (*1, 2*), and a subset
27 of such TCRs have been advanced into clinical trials (*3-5*). The most desirable TCR-T cell therapies
28 target antigens are tumor-specific, contribute to and/or are essential to the malignant phenotype, and well-
29 presented by the tumor being targeted. Mutant KRAS is the most common driver oncogene in human
30 malignancies (*6*), frequently mutated in pancreatic, colon, and lung cancers. 83% of gain-of-function
31 KRAS mutations result from a change in the glycine amino acid at the 12th residue (*7*). In particular,
32 mutation of glycine to valine, among the most common KRAS mutations in tumors (e.g., in 28.3% of all
33 pancreatic cancers (*8*)), has been postulated to create an epitope ($KRAS_{G12V}$, residues 5-14) presented on
34 tumor cells by HLA-A2 (*9*), the most common Class I allele worldwide (*10*). As tumors often become
35 oncogene-addicted to G12-mutant KRAS (*11*), these mutations are unlikely to be lost or revert to wild
36 type. In pursuit of G12 mutant KRAS as an oncologic target, drugs have recently been developed
37 targeting $KRAS_{G12C}$ by creating a covalent disulfide bond with the mutant cysteine residue. These drugs
38 have yielded promising response rates of 40-50%, but tumors rapidly develop resistance via mechanisms
39 such as structural KRAS mutations outside of G12 that cause steric hindrance of drug activity,
40 amplification of *KRAS* expression, and/or enhancement of downstream oncogenic signaling (*12, 13*); as a
41 result, median progression-free survival remains at about 6.5 months, with no evidence of cures (*14, 15*).
42 Thus, additional strategies for targeting mutant KRAS are needed. The ability to target epitopes
43 containing G12 mutations of KRAS with TCR-T cell therapy would provide an orthogonal strategy for
44 treating mutant KRAS-expressing tumors.

45 TCRs targeting KRAS epitopes containing a mutation at G12 presented by several HLA alleles
46 including HLA-A3 (*16*), HLA-A11 (*4, 17*), and HLA-C8 (*18*) have been reported to exhibit therapeutic
47 efficacy (*4, 19*). However, accessibility to this therapeutic strategy is limited by the low frequency of
48 these alleles in the US (e.g., 20–24% for HLA-A3 and less frequent for HLA-A11 and HLA-C8) (*20*). In
49 the US, HLA-A2 is the most common allele (47.6% (*21*)); the annual incidence of $HLA\text{-}A2^{+}$, mutant
50 KRAS cancers can be estimated to be 93,000 in the United States alone. Thus, targeting an A2-restricted

51 KRAS epitope would enable therapy for a far more substantial fraction of the population. However,
52 defining an A2-restricted KRAS epitope has proven problematic, including difficulties confirming within
53 the sensitivity of mass spectrometry (MS) that an A2-restricted epitope spanning the G12 position is
54 present in the immunopeptidome (*22, 23*). However, $KRAS_{G12V}$ does have epitopes predicted to bind well
55 to HLA-A2, particularly residues 5-14 (KLVVVGAVGV) (*9, 24*). As MS has been able to isolate G12V-
56 containing epitopes and other mutant KRAS epitopes from other HLA alleles (*23*), it has been presumed
57 the HLA-A2 epitope may not be naturally processed and/or efficiently presented by HLA-A2 (*22, 23*).
58 Several mechanisms may cause defective processing or presentation of a predicted epitope,
59 leading to immune evasion. Examples include differential expression of proteasome subunits that can
60 alter processing of a protein into an epitope (*25*), defective transportation of a processed epitope to the
61 endoplasmic reticulum for binding to MHC I (*26*), and deficiencies in MHC I expression or structure (*27*).
62 Additionally, proteins can undergo post-translational modifications (PTMs), and presentation of an
63 epitope containing a PTM can result in complete (*28*) or partial abrogation of epitope binding or
64 recognition by a TCR reactive to the unmodified epitope. Such changes include oxidation (*28*),
65 nitrosylation (*28*), methylation (*29*), phosphorylation (*30*), and glycosylation (*31*). Some PTMs may also
66 be more prevalent in tumors as a consequence of malignant transformation and enzyme dysregulation (*32,*
67 *33*). PTMs do occur in mutated KRAS (*34*), and could interfere with detection of an HLA-A2-presented
68 KRAS epitope by MS due to an altered migration pattern, contributing to the lack of consensus regarding
69 an A2 epitope.
70 Identifying a targetable epitope with a PTM for $KRAS_{G12V}$ is challenging due to experimental and
71 analytical limitations of MS in detecting PTMs (*35-37*), such as introduction of confounding chemical
72 artifacts (*37*), and PTMs have generally been overlooked when predicting epitopes for therapeutic TCR
73 development (*38*). For the KRAS protein, PTMs are known to occur in both the C-terminal region, which
74 are well-characterized for their signaling functions (*33, 39*), and the N-terminal region with methylation
75 of the lysine-5 side chain (*34*), which is included in the epitopes predicted to be presented by HLA-A2.

76 In this investigation, we demonstrate that methylation of the lysine-5 side chain in the $KRAS_{G12V}$
77 epitope that binds to HLA-A2 may interfere with targeting of $KRAS_{G12V}$ tumor cells by TCRs specific for
78 the unmodified epitope. Combining machine learning-based computational approaches to model
79 TCR:pMHC interfaces with high-throughput experimental screens, we developed translationally
80 promising TCRs that can target both methylated and unmodified epitopes, thereby providing broader anti-
81 tumor activity against HLA-A2$^+$, $KRAS_{G12V}^+$ tumor cells. Finally, we uncovered the potential role of a
82 protein canonically known to diminish histone methylation, SPT6 (*40*), in reducing methylation of the
83 $KRAS_{G12V}$ epitope. This may be targetable in tumor cells as a method to enhance immunologic
84 recognition by methylation-targeting TCR-T cells and exemplifies a potential synergistic strategy to
85 inhibit tumor evasion of T cell immunity.
86

87 # Results

88 <u>Post-translational modifications of the HLA-A2-presented $KRAS_{G12V}$ epitope alter its recognition by</u>
89 <u>MHC class I-restricted TCRs and prevent tumor cell killing.</u>

90 Computational prediction, by NetMHCPan 4.1 (*41*), of HLA-A2-presented $KRAS_{G12V}$ identified
91 several epitopes that specifically contain the G12V mutation (**Fig. S1a**). Among the top ten predicted
92 epitopes encompassing the full mutated KRAS protein, three contained the G12V mutation, and the
93 epitope consisting of residues 5-14 (i.e., KLVVVGAVGV) was predicted to bind with the highest avidity.

94 For our initial effort to develop HLA-A2-restricted TCRs targeting this peptide, we isolated
95 primary CD8$^+$ T cells from peripheral blood mononuclear cells (PBMCs) from HLA-A2$^+$ healthy human
96 donors and expanded epitope-reactive clonotypes by stimulation with autologous antigen-presenting cells
97 (APCs) pulsed with a synthetic $KRAS_{G12V}$ 5-14 peptide that lacked any PTMs (**Materials and Methods**).
98 We sorted cells with potentially high affinity for the $KRAS_{G12V}$ peptide as measured by binding limiting
99 concentrations of HLA-A2:$KRAS_{G12V(5\text{-}14)}$ tetramers. From the sorted cells, we then quantitated TCR
100 clonotypes using the ImmunoSEQ assay (Adaptive Biotech) and identified paired TCRa/TCRb sequences

101 using single cell RNA-seq. TCR clonotypes preferentially enriched within the sorted populations were
102 synthesized as codon-optimized P2A-linked constructs of TCRa and TCRb in a lentiviral backbone and
103 used to transduce $CD8^+$ T cells. The cells were stimulated with titrated concentrations of $KRAS_{G12V(5-14)}$
104 peptide, and the resulting IFNγ expression measured to assess functional avidities for this peptide (**Fig.**
105 **1a; Fig. S1b**). Two particularly high affinity TCRs were identified, TCR_{19} and TCR_2, with the former
106 exhibiting the highest functional avidity. However, in a coculture with the HLA-$A2^+$, $KRAS_{G12V}{}^+$
107 pancreatic adenocarcinoma cell line CFPAC1, $CD8^+$ T cells transduced with TCR_{19} unexpectedly
108 demonstrated poorer inhibition of tumor growth compared to T cells transduced with TCR_2 (**Fig. 1b**),
109 whereas TCR_{19} conversely demonstrated better inhibition than TCR_2 of DAN-G tumor cell growth, which
110 are also HLA-$A2^+$ and $KRAS_{G12V}{}^+$.

111 The reasons for this discrepancy between TCR functional avidities for $KRAS_{G12V(5-14)}$ and killing
112 of different tumor cells were unclear. One explanation could be alloreactivity rather than tumor antigen
113 specificity. For killing of CFPAC1 cells, alloreactivity to this cell line by TCR_2 would not necessarily
114 have been predicted by measuring the dose response of cells with this TCR to peptides presented by
115 another antigen-presenting cell. However, TCR_2 did not induce a reaction against any of the Class I HLA
116 alleles found on CFPAC1 cells on other targets not expressing mutant KRAS (HLA-A2, A3, B35, B73,
117 C4, C15; **Fig. S1c**). Alternatively, TCR_{19} killing of DAN-G cells could reflect allorecognition, but similar
118 studies did not detect recognition of the alleles on DAN-G by TCR_{19}. Thus, alloreactivity was an unlikely
119 explanation. We therefore hypothesized that, while both of these HLA-$A2^+$ $KRAS_{G12V}{}^+$ tumor cells may
120 be presenting the epitope, one may be presenting it in a modified form, and that there was differential
121 recognition of the modified and unmodified peptide by each TCR.

122 Before more closely examining the presence of PTMs, we wanted to confirm that the predicted
123 primary sequence, $KRAS_{G12V}$ 5-14, is in fact efficiently generated by proteasomal cleavage and presented
124 by HLA-A2. To accomplish this, we used the ARTEMIS technology, which entails MS-based
125 identification of MHC I epitopes bound to a secreted single-chain dimer (SCD) of the selected HLA I
126 allele (*42*) (**Materials and Methods**). This provides an abundant source of easily purified peptide-bound

127 Class I molecules, can detect the majority of peptides that get endogenously processed and loaded on
128 Class I in the ER, and overcomes the challenge of identifying the limited amount of peptide specifically
129 presented on the cell surface by an individual Class I allele using MS (*42*). We established an ARTEMIS
130 system in the 293F cell line, which supports exceptionally abundant protein expression compared to other
131 mammalian cell lines (*43*). 293F cells were lentivirally transduced to express a secreted HLA-A2 SCD as
132 well as a truncated version of the $KRAS_{G12V}$ protein (amino acids 1–100 to render the protein
133 nonfunctional but preserve the N-terminal portion of the protein that contains the G12V mutation), to
134 increase the availability of $KRAS_{G12V}$-originated peptides that contain the G12V mutation for binding to
135 HLA-A2. Three HLA-A2-presented KRAS peptides were identified by ARTEMIS, including the
136 $KRAS_{G12V}$ 5-14 peptide, which was the only HLA-A2-presented peptide containing the mutated G12V
137 residue (**Fig. 1c**). These results confirmed that the 5-14 epitope is a dominant product of $KRAS_{G12V}$
138 antigen processing and presentation associated with HLA-A2 and is the correct peptide sequence to target
139 with TCRs.

140 Given the known dysregulation of methylation processes in mutant KRAS-driven cancers (*32, 33,*
141 *44, 45*), and the previously detected lysine-5 side chain methylation of Ras family proteins (*34*), we
142 considered the possibility that the $KRAS_{G12V}$ 5-14 epitope presented by tumor cells contains some level of
143 methylation or other post-translational modification. Having confirmed the primary sequence of the
144 epitope, we hypothesized that DAN-G cells were presenting $KRAS_{G12V}$ 5-14 epitope such that some
145 combination of lysine-5-methylated and unmodified epitope was likely being presented. In turn, the
146 presence of the weakly recognized, modified epitope may have limited the recognition of these tumor
147 cells by TCR_2 and TCR_{19}, thereby limiting tumor killing. However, as 293F cells may not have the same
148 protein methylation machinery active in DAN-G, we attempted to design ARTEMIS in DAN-G cells.
149 Unfortunately, due to the low cell density of cultured DAN-G cells and lower level of protein expression
150 compared to 293-based ARTEMIS cells, we did not detect sufficient levels of peptide to identify the
151 methylated epitope. Therefore, to search for differences in methylation activities that can lead to increased
152 methylation within KRAS in DAN-G cells, we also performed immunoprecipitation of whole-protein

153 KRAS from DAN-G and CFPAC1 cells, followed by liquid chromatography-MS. This revealed that in
154 DAN-G cells, but not in CFPAC1 cells, lysine side chain trimethylation was present at lysine-16 (**Fig.**
155 **S1d**), representing full replacement of all hydrogens of the amine group by methyl groups. No peptides
156 containing lysine-5 of KRAS were able to be recovered or detected in this data set, likely due to the
157 cleavage of the KRAS protein by trypsin immediately after lysine-5 during sample processing for MS
158 (*46*), producing a short 5-mer peptide that would be difficult to detect with our MS technology. Thus,
159 while we could not directly confirm the presence of a lysine-5-methylated peptide, a pattern of increased
160 KRAS lysine methylation was evident in DAN-G cells. Additionally, previous reports clearly
161 demonstrated methylation of KRAS at lysine residues (*33, 34*) including dimethylation at lysine-5. Lysine
162 side chain methylation may exist as mono-, di-, or trimethylation, with the former two states being
163 intermediate degrees of full methylation.

164 To determine whether the $KRAS_{G12V(5-14)}$ peptide with lysine-5 methylation binds to HLA-A2
165 with comparable affinity as the unmodified peptide, we assessed the stability of HLA-A2:$KRAS_{G12V}$
166 pMHC complexes with or without lysine-5 side chain methylation. T2 cells are deficient in Transporter
167 Associated with Antigen Processing (TAP) protein and express few properly folded Class I molecules on
168 the cell surface (*47*). Pulsing T2 cells with exogenous peptide can stabilize the conformation of HLA-A2
169 molecules on the cell surface, resulting in enhanced surface expression that correlates with peptide
170 affinity for HLA-A2 (*47*). We pulsed T2 cells with $KRAS_{G12V(5-14)}$ with or without methylation and
171 measured the resulting surface expression of HLA-A2 (**Materials and Methods; Fig. S1e**). Compared to
172 untreated control cells, HLA-A2 surface expression was higher when T2 cells were pulsed with the
173 $KRAS_{G12V(5-14)}$ peptide. Moreover, pulsing with the same peptide containing different degrees of lysine-5
174 methylation further increased A2 expression, indicating that methylation may enhance the stable
175 presentation of the epitope. Although the unmodified peptide was recognized well by both TCRs, there
176 were large differences in the abilities of the TCRs to recognize the methylated epitope (**Fig. 1d**).
177 Therefore, differential lysine 5-methylation may explain the disparities in the killing of different tumor
178 cells observed with these TCRs.

179 In addition to the 10-mer $KRAS_{G12V}$ 5-14 sequence detected from ARTEMIS, a 9-mer
180 (LVVVGAVGV) is another predicted epitope containing the G12V mutation that bind HLA-A2 (**Fig.**
181 **S1a**), and a previous study has also reported peptide splicing to produce an HLA-A2-presented epitope
182 containing residues 5-6/8-14 of $KRAS_{G12V}$ (*24*). To rule out recognition of these alternative epitopes by
183 the TCRs and to test recognition of methylated epitope, we synthesized these epitope variants as well as
184 $KRAS_{G12V(5-14)}$, including this peptide post-translationally modified at lysine-5. To determine the
185 functional avidities of the TCRs for these variant epitopes, we stimulated T cells expressing TCR_2 or
186 TCR_{19} with these epitopes as presented by HLA-A2 and measured resulting IFNγ expression (**Fig. 1d**).
187 Indeed, while both TCR_2 and TCR_{19} recognized unmethylated $KRAS_{G12V}$ 5-14 to similar degrees, only
188 TCR_{19} produced a response to the peptide with methylation of the amine group on the side chain of
189 lysine-5. Other forms of the G12V-containing epitope which had lower predicted binding ability from
190 NetMHCPan 4.1 (residues 6-14 or 5-12), and an alternatively spliced peptide $KRAS_{G12V}$ 5-6/8-14
191 previously suggested to be processed (*24*), also did not elicit a response from the TCRs. Thus, the DAN-
192 G cell line may be modifying a fraction of $KRAS_{G12V}$ protein or its resulting epitopes with lysine-5 side
193 chain methylation, such that the epitope presented by this tumor cell could not be recognized by TCR_2.
194 The presence of lysine-5 methylation is consistent with prior findings examining methylation of RAS
195 family proteins, including KRAS (*34*), and is consistent with the known dysregulation of protein
196 methylation in mutant KRAS-driven cancers (*32, 33*).
197 Based on the evidence supporting contribution of a lysine-5 methylated peptide to TCR
198 recognition of the HLA-A2-presented $KRAS_{G12V(5-14)}$ epitope, we sought to identify structural changes
199 that may occur as a result of such methylation. Using the Rosetta (*48*) protein structure modeling tool, we
200 introduced monomethylation, dimethylation, and trimethylation to the lysine-5 side chain and evaluated
201 the resulting changes in peptide positioning in the MHC cleft. This computational pipeline indicated that
202 methylation of the lysine-5 side chain within HLA-A2-presented $KRAS_{G12V(5-14)}$ induces shifts of the
203 positioning of the amine group of this side chain that could affect TCR recognition of the epitope (**Fig.**
204 **1e**): in the unmodified peptide, the amine group of the lysine-5 side chain protrudes out of the MHC I

205 cleft potentially into close proximity to the TCR chain, suggesting it may serve as a contact point between
206 the TCR and pMHC complex. Monomethylation leads to displacement of the amine group deeper into the
207 MHC I cleft by the methyl group, which is further pronounced by dimethylation or trimethylation,
208 potentially explaining the observed impact of methylation on the recognition of this pMHC complex by
209 TCR_2 or TCR_{19}.

210 To evaluate the relative contribution of the lysine-5 residue to binding of each TCR to the HLA-
211 A2-presented $KRAS_{G12V}$ epitope, we performed alanine scans, in which each residue of the HLA-A2-
212 presented epitope is sequentially substituted with the small, neutral alanine amino acid. Each alanine
213 mono-substituted epitope was then used to pulse antigen-presenting cells to stimulate $CD8^+$ T cells
214 expressing TCR_2 or TCR_{19}, and IFNγ was then measured to determine if recognition of the whole epitope
215 is impacted by the alanine substitution (*49*), which would imply that the substituted amino acid is a
216 relevant contact point for the TCR. Residue 11 of the 5-14 epitope, which is already alanine, was
217 alternatively substituted with threonine or glycine. At peptide concentrations of 0.1 μg/ml, the analysis
218 revealed that substitution of lysine-5 to alanine reduced the response to the epitope from 67.9%
219 responsive cells to 2.45% for TCR_2 (**Fig. 1f**), suggesting that TCR_2 is sensitive to changes at that position
220 of the epitope. The pMHC complex with $KRAS_{G12V}$ epitope, as modeled by Rosetta, also indicates
221 protrusion of the lysine-5 side chain out of the groove of HLA-A2 in the direction where it could interact
222 with a TCR (**Fig. S1f**, which uses the same models as **Fig. 1e** but is rotated for display from a perspective
223 showing this protrusion more clearly). By contrast, the alanine scan for TCR_{19} revealed high tolerance for
224 amino acid substitutions at most positions of the $KRAS_{G12V}$ epitope, which may explain its recognition of
225 methylated lysine-5 but suggesting it would be promiscuous and less suitable as a potentially therapeutic
226 TCR to modify for pursuing improvements (**Fig. 1f**).
227

228 <u>A rationalized mutagenesis approach can be used to generate TCRs that recognize methylated $KRAS_{G12V}$</u>
229 <u>epitope to improve targeting of tumor cells.</u>

230 Identifying TCRs that can recognize lysine-5 side chain mono-, di-, and/or trimethylation of the
231 $KRAS_{G12V}$ 5-14 peptide alone or in addition to the unmodified version of that peptide could potentially
232 increase the ability to therapeutically target HLA-A2$^+$ tumors with the $KRAS_{G12V}$ mutation. To generate
233 new TCRs that can target the peptide with the three different degrees of lysine-5 methylation, we first
234 explored a strategy to mutagenize the CDR3α region of an existing TCR, TCR_2, which recognizes the
235 unmodified peptide with high functional avidity and specificity for the $KRAS_{G12V}$ epitope, to determine if
236 we could broaden peptide recognition to include methylated variants without acquisition of more general
237 promiscuity.

238 To determine the region of this TCR most likely to interact with the methylation site, we
239 developed a new computational structural prediction workflow (**Fig. S1g**). We first used Alphafold (*50*),
240 which utilizes deep learning-based approaches to predict the structure of the TCR:pMHC complex
241 without any PTMs, as the latter are not modeled well by Alphafold. We fed the output into Rosetta, which
242 utilizes physics-based energy functions to allow for modeling additional molecular changes to that
243 structure, such as introducing PTMs to the epitope, and then readjusting the structural prediction. Our
244 workflow, performed on the existing TCR_2 that recognized the unmodified $KRAS_{G12V}$ 5-14 peptide
245 presented by HLA-A2, revealed a core sequence within the CDR3α region most likely to be in close
246 proximity to the lysine-5 side chain and any potential methylation modifications to this residue (**Fig. 2a**).

247 Using the structural model as the guide to the most relevant region, we created a rationalized
248 mutagenesis library of this computationally identified core CDR3α sequence. Library-transduced CD8$^+$
249 Jurkat cells were stimulated to detect TCR clonotypes that recognized differently modified variants of the
250 $KRAS_{G12V}$ 5-14 peptide (**Materials and Methods**). Library-transduced T cells were analyzed for binding
251 to unmethylated or lysine-5-methylated $KRAS_{G12V(5\text{-}14)}$ peptide. A broad spectrum of reactivity towards
252 one or both of these peptides was observed, confirming that the computationally determined CDR3α
253 sequence plays a key role in recognition of the putative lysine-5 methylation site by TCR_2. We identified
254 several distinct clonotypes able to bind to only the unmethylated peptide (e.g., TCR_{EDVA}), to a
255 combination of unmethylated and mono/di/trimethylated epitopes (e.g., TCR_{4UM}, TCR_{EDST}, TCR_{EDRS}), or

256 to only methylated peptides (TCR_{TGNT}; **Fig. 2b–c**), which were sequenced to identify the corresponding
257 mutant variants. New constructs were then generated expressing these mutant variant TCRs. A dose
258 response assay with $CD8^+$ T cells transduced with each mutant variant was performed using the
259 unmethylated and methylated $KRAS_{G12V}$ epitopes individually. Some mutagenized TCRs, when
260 compared to TCR_2, had improved recognition of the methylated epitope (**Fig. 2d**). A dose response assay
261 revealed no significant acquisition of recognition of wild type KRAS 5-14 or the alternative $KRAS_{G12D}$ 5-
262 14 epitope by the mutagenized TCRs compared to TCR_2 (**Fig. S2a**). Thus, changes in amino acids within
263 only this computationally identified core CDR3α sequence were able to alter the TCR's pattern of
264 recognition for peptides with PTMs (**Fig. S3a–b**) without altering recognition of non-G12V KRAS
265 epitopes. For TCR_{EDST}, labeled as such for the mutagenized 'core' CDR3α sequence, the amino acids in
266 closest proximity to the lysine-5 side chain of the HLA-A2-presented $KRAS_{G12V}$ epitope were aspartate
267 and serine. These amino acids are negatively charged and polar, respectively, allowing for electrostatic or
268 hydrogen bonding interactions with the lysine-5 side chain amine group of the $KRAS_{G12V}$ epitope. While
269 methylation introduces a hydrophobic methyl group, the polar nature of the amino acids on this TCR may
270 still allow for binding to the lysine side chain.

271 We then tested whether $CD8^+$ T cells expressing the TCR variants with enhanced binding to
272 methylated peptides could efficiently recognize and kill $KRAS_{G12V}$-expressing tumor cells. In coculture
273 with $KRAS_{G12V}^+$ HLA-$A2^+$ tumor cells, $CD8^+$ T cells expressing TCR_{EDST} or TCR_{EDRS}, which recognize
274 unmethylated and methylated $KRAS_{G12V}$ epitopes, demonstrated improved killing of DAN-G cells, which
275 likely presents methylated and unmethylated $KRAS_{G12V(5\text{-}14)}$, and retained similar killing of CFPAC-1
276 cells compared to TCR_2 (**Fig. 2e**). Consistent with the lack of recognition of wild type $KRAS_{5\text{-}14}$ or
277 $KRAS_{G12D(5\text{-}14)}$ in the peptide dose response assay, these TCRs did not inhibit growth of HeLa cells, which
278 express only wild type $KRAS_{5\text{-}14}$, or of Panc1 cells, which express $KRAS_{G12D}$ (**Fig. S2b**). Taken together,
279 mutagenesis of the originally naturally isolated TCR_2 yielded new TCRs recognizing different
280 combinations of unmodified and varyingly methylated $KRAS_{G12V}$ epitopes without increasing "off-target"
281 recognition of G12D or wild type epitopes of KRAS.

282 A critical concern with TCRs deployed for ACT is that specificity needs to be limited only to the
283 intended targets to avoid off-target toxicities, which is of increased concern after a naturally isolated TCR
284 is mutagenized. To further evaluate the specificity of the selected TCRs, we again performed alanine
285 scans of the target epitope for recognition by the mutagenized TCRs in Jurkat reporter cells expressing
286 CD8ab, TCR_2 or mutagenized TCR (TCR_{4UM}, TCR_{EDST}, TCR_{EDRS}, TCR_{TGNT}, or TCR_{EDVA}), and the Nur77-
287 GFP reporter gene as a specific marker of TCR signaling(*51*). After pulsing with 0.1 μg/ml peptide
288 concentrations (~106 nM for this epitope), a concentration high enough to induce complete responses to
289 the original $KRAS_{G12V\ (5\text{-}14)}$ epitope, and with tolerance to a change defined as retaining Nur77-GFP
290 reporter expression in >35% of cells that respond to the original epitope, there were distinct positions
291 common to both the unmethylated and methylated versions of the epitope that tolerated amino acid
292 replacements and remained stimulatory (**Fig. S2c**). For TCR_2, TCR_{EDST}, and TCR_{EDST}, the overall
293 tolerance pattern was K-x-x-V-V-x-A-x-x-x, with x signifying tolerance for an alanine substitution at that
294 position; among these three TCRs, TCR_{EDST} exhibited the lowest tolerances. Compared to these TCRs,
295 TCR_{4UM} demonstrated greater tolerance for substitutions, and TCR_{TGNT} and TCR_{EDVA} showed lower
296 tolerances but demonstrated less effective tumor control. Thus, TCR_{4UM}, TCR_{TGNT}, and TCR_{EDVA} were
297 determined to be less suitable as candidate therapeutic TCRs. Notably, while some TCRs could recognize
298 both unmethylated and methylated versions of the lysine-5 side chain, replacement of lysine-5 with
299 alanine led to a loss of recognition of the presented peptide. The diminution of recognition was greater
300 than observed with substitutions at other peptide positions, suggesting this lysine amino acid remained a
301 major contact point for the mutagenized TCRs as it did for TCR_2. A scan of the human peptidome for
302 epitopes that accommodated any substitution at these permissive residues yielded $PLD3_{396\text{-}405}$, $MIGA1_{74\text{-}}$
303 $_{83}$, $NAGPA_{276\text{-}285}$, $K/N/HRAS_{5\text{-}14}$, $RSLBB_{35\text{-}44}$, $CFA61_{23\text{-}32/607\text{-}616/667\text{-}676}$, $CUL9_{635\text{-}644/745\text{-}754}$, $CLCN6_{80\text{-}89}$, and
304 $MACOI_{33\text{-}42}$ as potential off-target hits. These peptides were synthesized and used to stimulate T cells
305 expressing the TCR. Relative to HLA-A2-presented $KRAS_{G12V}$ 5-14, all of the selected TCRs exhibited
306 reduced responses against these peptides at 0.1 μg/ml concentration (**Fig. S2d**), suggesting the
307 mutagenized TCRs had not acquired significant promiscuity compared to the original TCR_2. Additionally,

308 for TCR_2 and TCR_{EDST}, at more physiologic concentrations of 0.01 μg/ml (~10.6 nM), these peptides
309 elicited response rates of <6% compared to 18–19% for the $KRAS_{G12V}$ epitope, as measured by
310 percentage of cells expressing IFNγ (**Fig. S2e**).
311
312 Stimulation of primary T cells with selected peptides followed by clonal expansion reveals TCRs from
313 healthy donor repertoires that recognize methylated $KRAS_{G12V}$ epitope and can target tumor cells.
314 The TCRs generated from the mutagenesis approach were able to specifically target and
315 effectively kill HLA-A2 tumor cell lines expressing $KRAS_{G12V}$ with PTMs. However, such TCRs have
316 not been naturally vetted by the thymic selection process, and thus may pose a risk for cross-reactivity
317 with other peptides from the human proteome despite the safety testing based on the alanine scan. Thus,
318 to identify TCRs from normal peripheral repertoires potentially capable of binding to the methylated
319 KRAS epitopes, primary human T cells from healthy donor PBMCs were stimulated with $KRAS_{G12V}$
320 peptides including unmethylated, mono-, di-, and tri-methylated lysine-5, and responding T cells were
321 sort purified based on specific binding to individual HLA-A2:PTM-containing $KRAS_{G12V}$ 5-14 tetramers
322 at limiting peptide concentrations. Quantitative TCR repertoire analysis was performed on the purified
323 populations, and highly enriched TCR clonotypes were synthesized and expressed in primary $CD8^+$ T
324 cells (**Materials and Methods; Fig. S4a, b**).
325 As measured by IFNγ expression by TCR-transduced T cells after exposure to unmethylated and
326 methylated $KRAS_{G12V}$ epitopes presented by HLA-A2, these TCRs exhibited dose response patterns
327 specific to the G12V mutation, responded to methylated and/or unmethylated peptides, and did not
328 recognize wild type or G12D mutant epitopes (**Fig. 3a**). The functional avidities of these TCRs,
329 $TCR_{A2UoM1-1}$, $TCR_{A2UoM1-2}$, and $TCR_{A2UoM1-4}$, for the unmethylated and monomethylated peptides were
330 comparable to those of the mutagenesis-derived TCRs, in particular TCR_{EDST} which exhibited superior
331 killing of DAN-G cells and strong recognition of unmethylated and methylated $KRAS_{G12V}$ epitopes.
332 Among the TCRs that exhibited the strongest recognition of methylated and unmodified peptides,
333 coculture with tumor cells of $CD8^+$ T cells expressing $TCR_{A2UoM1-1}$ demonstrated superior killing

334 compared to T cells expressing TCR_2 of the HLA-A2$^+$ $KRAS_{G12V}^+$ DAN-G tumor cell line, inferred to
335 present methylated and unmethylated $KRAS_{G12V}$ 5-14 (**Fig. 3b**). $TCR_{A2UoM1-1}$ also exhibited similar killing
336 as the other TCRs against CFPAC1, which presumably presents unmethylated $KRAS_{G12V}$ 5-14.
337 $TCR_{A2UoM1-1}$ did not recognize titrated doses of HLA-A2-presented wild type KRAS 5-14 or $KRAS_{G12D}$ 5-
338 14 (**Fig. S4c**) but did exhibit some inhibition of HLA-A2$^+$ tumor cell lines expressing either wild type or
339 G12D KRAS (**Fig. S4d**), suggesting that there may be some broader targeting. However, an alanine scan
340 with $TCR_{A2UoM1-1}$ demonstrated very limited tolerance for amino acid substitutions within the $KRAS_{G12V}$
341 5-14 epitope (**Fig. S4e**), such that the only potential match in the human peptidome (using the same
342 criteria as our previous alanine scans) was $EPIPL_{1948-1957}$. A dose response assay performed with this
343 peptide revealed no recognition by this TCR (**Fig. S4f**), affirming its highly selective specificity.
344 Structural modeling of $TCR_{A2UoM1-1}$ revealed a CDR3α sequence that had amino acids aspartate
345 and serine in closest proximity to the lysine-5 side chain including the differently methylated versions
346 (**Fig. 3c**). These TCR amino acids are identical to what was identified in the mutagenized TCR_{EDST}, and
347 thus may allow for close interaction with both methylated and unmethylated lysine-5 of the $KRAS_{G12V}$
348 epitope by both TCRs.
349
350 <u>SPT6 is involved in the mechanism for demethylation of lysine-5 of the $KRAS_{G12V}$ epitope in tumor cells</u>
351 <u>and may be a target for creating presentation of a stable epitope with a methylation-specific TCR.</u>
352 We next sought to determine potential genes involved in $KRAS_{G12V}$ epitope methylation. To
353 address this, we performed a CRISPR-Cas9 library screen targeting genes canonically known to be
354 involved in DNA or protein methylation (**Materials and Methods; Fig. 4a**). The library was transduced
355 into the DAN-G cell line, which is inferred to express the methylated $KRAS_{G12V(5-14)}$ epitope and is
356 recognized by TCRs that have specificity for the methylated epitope but not effectively by TCRs only
357 specific for the unmodified epitope. Tumor cells were collected before and after co-culture with
358 methylation-responsive TCR-T cells (TCR_{EDST}) and TCR-T cells that preferentially target unmodified
359 KRAS (TCR_2), and the frequencies of each gRNA in surviving tumor cells were determined. TCR_{EDST}

360 was chosen as the methylation-sensitive TCR for this comparison because it differs from TCR_2 only in its
361 ability to recognize methylated lysine-5. This analysis revealed reduced recovery of certain gene
362 knockouts when cocultured with TCR_{EDST}, but not when cocultured with TCR_2, suggesting that the
363 knocked-out gene conferred a survival disadvantage for tumor cells that might reflect increased
364 presentation of the methylated epitope. In contrast, a higher frequency of gRNAs targeting a given gene in
365 the same comparison of cocultures would mean that the knockout conferred a survival advantage, thereby
366 providing a means of immunological escape from the TCR_{EDST}-T cells by diminishing presentation of the
367 methylated epitope.

368 In the gene knockout screen, DAN-G cells with *SUPT6H* knockout (encoding the SPT6 protein)
369 were the single most depleted knockout when comparing tumor cells cocultured with the methylation-
370 targeting TCR_{EDST}-T cell to the non-methylation-targeting TCR_2-T cell coculture (**Fig. 4b**). This suggests
371 that SPT6 expression decreased methylation of this epitope. SPT6 is canonically known as a negative
372 regulator of histone lysine methylation (*40*). From our data, SPT6 appears to have a non-canonical role as
373 an inhibitor of lysine methylation on the $KRAS_{G12V}$ epitope.

374 To further investigate the enhanced effectiveness of methylation-targeting TCR-T cells
375 specifically against SPT6-deficient DAN-G cells, we created a *SUPT6H* knockout DAN-G cell line.
376 Successful knockout was verified via long-read sequencing of the targeted genomic region (**Fig. S5a**).
377 Coculture of the *SUPT6H*-knockout DAN-G cells with $CD8^+$ T cells transduced either with TCR_{EDST},
378 which targets both unmethylated and methylated $KRAS_{G12V}$ epitope, or with TCR_2, which only effectively
379 targets the unmethylated $KRAS_{G12V}$ epitope, affirmed that knockout of *SUPT6H* increased susceptibility
380 to killing by T cells expressing either TCR_{EDST} or $TCR_{A2UoM1-1}$ which also targets the methylated epitope
381 (**Fig. 4c**). Additionally, the knockout did not increase killing by T cells expressing the methylation-
382 unresponsive TCR_2. Relative to the original DAN-G cells, *SUPT6H* knockout did not increase HLA-A2
383 expression (**Fig. S5b**) and did not change KRAS expression levels (**Fig. S5c**), indicating that the effect of
384 *SUPT6H* knockout was not due to changes in total epitope presentation levels but rather due to changes in
385 the PTM composition of the epitope.

386 Data from The Cancer Genome Atlas (TCGA) show that loss-of-function mutations of *SUPT6H*
387 specifically within the $KRAS_{G12V}$ mutant cancer patient population lead to increased survival compared to
388 the *SUPT6H*-mutant patient population as a whole (**Fig. 4d**). This mutation-specific behavior may suggest
389 that the methylated $KRAS_{G12V}$ epitope is more spontaneously immunogenic in the context of a naturally
390 occurring TCR repertoire, which would be consistent with the more stabilized cell surface expression of
391 the HLA-A2:$KRAS_{G12V}$ pMHC complex when the epitope is methylated compared to unmethylated, as
392 we described earlier (**Fig. S1e**).

393

394 # Discussion

395 Development of effective ACT using TCRs requires accurate identification of the epitopes
396 specifically presented by the targeted tumor, which can become increasingly difficult in the context of
397 PTMs. In this study, we have demonstrated, using two approaches, the ability to isolate/generate TCRs
398 that recognize and target PTMs that can alter the immunogenicity of a tumor epitope in a therapeutically
399 consequential manner. Deep learning-guided mutagenesis made it feasible to refine a potentially
400 promising TCR targeting an HLA-A2-presented $KRAS_{G12V}$ epitope into one able to target both post-
401 translationally modified and unmodified variants of the epitope, thereby achieving improved killing of
402 HLA-$A2^{+}$, $KRAS_{G12V}$ tumor cell types. We also generated TCRs that can achieve similar activity by
403 selectively expanding rare clonotypes reactive against modified and unmodified $KRAS_{G12V}$ peptide
404 variants from healthy donor-derived primary T cell populations, thereby selecting for TCRs that have
405 undergone the thymic central tolerance process, meaning they are less likely to react against self-antigens
406 and may offer a safer therapeutic profile. For tumor cells that might present the unmodified $KRAS_{G12V}$
407 epitope together with a mix of variants with different degrees of a lysine-5 methylation, our data suggests
408 that therapeutic TCRs designed or selected to target a wide range of these variants should prove more
409 effective at killing a larger subset of $KRAS_{G12V}$-expressing tumor cells, and preclude immune evasion
410 driven by altered or variable KRAS lysine methylation.

411 Computational prediction of TCR specificity against pMHC complexes has recently experienced
412 significant improvements (*52*), but purely computational approaches still require experimental validation
413 to determine whether TCR specificity is sufficiently high to be safe and effective for antitumor therapy.
414 Predicting the three-dimensional architecture between a pMHC complex and TCR has the potential to
415 provide insights for experimentally modifying and improving the affinity/specificity of the TCR for the
416 pMHC based on proposed contact points, orientation of a peptide within the pMHC, and orientation of the
417 TCR to that complex. However, the structure of the TCR:pMHC complex has historically been difficult to
418 accurately determine computationally due to the still somewhat limited number of experimentally
419 validated structures of TCR:pMHC interactions from which to base new predictions, the bias of
420 prediction models to overfit based on existing common epitopes, and the lack of negative control data (*53,*
421 *54*). Recent innovations in computational protein structure prediction, including Alphafold, have allowed
422 for improved accuracy (*53*). Nonetheless, Alphafold does not yet support the structural prediction of
423 changes resulting from PTMs due to the lack of available structural data for training that includes PTMs
424 (*55*). Alternatively, Rosetta utilizes physics-based energy functions to optimize protein structures, which
425 better accommodates integration of PTMs into protein structure prediction (*56*). Thus, in this
426 investigation, we combined these two pipelines into one prediction to yield a more precise guide that
427 accurately identified pMHC contact sites within the TCR CDR3 sequences that could subsequently be
428 modified through saturation mutagenesis to specifically enhance TCR association with post-
429 translationally modified peptide within the pMHC complex. This strategy allowed us to develop new
430 TCRs that more effectively target HLA-A2^{+} KRAS$_{G12V}^{+}$ tumors, while maintaining TCR specificity for
431 mutant KRAS.

432 Developments in MS technology, including newer technology with greater sensitivity, have
433 allowed for its use to identify MHC class I-restricted T cell epitopes (*35, 42*). We used such MS to
434 characterize the primary sequence of the HLA-A2-presented KRAS$_{G12V}$-containing epitope in this study,
435 analogous to previous studies that identified mutant KRAS epitopes presented by other MHC I alleles (*4,*
436 *9, 19*). These MS-based studies have been important for the development of potentially therapeutic TCRs

437 for mutant KRAS tumors. However, MS can remain unreliable for detecting PTMs. The large size of the
438 immunopeptidome presented by the multiple MHC I and II alleles expressed by a tumor, the often-
439 reduced level of MHC expression by tumor cells, the low yield fraction of protein capture, and low
440 expression of some proteins of interest can result in low and inadequate sensitivity for detection of a
441 specific epitope and any associated PTMs (*35*). As a result, MS-based workflows can benefit from
442 maximizing protein expression and MHC capture as we did with ARTEMIS in this study. Additionally,
443 the introduction of chemical artifacts during sample processing, such as oxidation (*37*), may confound
444 whether a detected PTM is genuine or not, and PTMs that are not suspected prior to analysis to be on a
445 peptide may result in missing the detection of that peptide (*36*). To bypass these difficulties associated
446 with epitope detection and probe for a specific PTM on a presented epitope, TCRs with distinct PTM-
447 peptide recognition patterns may be used as an alternative to MS, as these TCRs will elicit T cell
448 activation in response to a target presenting distinct PTMs and can serve as a very sensitive assay for the
449 presence or absence of the PTM.

450 Based on the results of our efforts to generate TCRs targeting HLA-A2-presented $KRAS_{G12V}$,
451 TCR_{EDST} and $TCR_{A2UoM1-1}$ appear to be two promising candidates for further development as therapeutic
452 TCRs. The former was generated by mutagenesis of an existing TCR that naturally recognized an
453 unmodified epitope derived from mutant KRAS, whereas the latter was identified by selection from a
454 healthy donor's TCR repertoire. The mutagenesis approach allows for generation of TCRs that may not
455 be present in normal repertoires and that have increased affinity for the target. However, because these
456 TCR sequences are mutated from a TCR naturally existing in the repertoire, they have not been naturally
457 screened during development against the self-immunopeptidome, and pose an elevated risk of off-target
458 activity in a therapeutic setting. Thorough testing for TCR recognition of cross-reactive targets *in vitro*, as
459 we have initiated with alanine scans followed by identification and testing of potential non-$KRAS_{G12V}$
460 targets in the proteome, should help to mitigate this problem. Additionally, such TCRs may be useful as
461 probes to identify the presence of particular PTMs on epitopes presented by different tumors. TCR
462 discovery from the repertoire of a healthy donor that has already been centrally thymically tolerated is

463 theoretically safer than TCRs generated by mutagenesis, but can be limited if the desired TCR clonotypes
464 are particularly rare within the repertoire or only of low affinity. Overall, we show that either approach is
465 feasible to generate potentially effective, therapeutic TCRs able to target a modified and/or unmodified
466 tumor antigen of interest.

467 Our findings with the histone methylation inhibitor SPT6 (*SUPT6H*) provide further evidence that
468 PTMs may be introduced by potentially non-canonical processes (*32, 57*), analogous to the non-canonical
469 methylation activity of SMYD3 that has been shown to impact other components of the KRAS signaling
470 pathway (*32*). From our findings, *SUPT6H* knockout in tumor cells enhances the efficacy of KRAS-
471 targeting, PTM-reactive, TCR-T cells. Diminishing SPT6 activity may provide another opportunity to
472 increase tumor immunogenicity, such as by combining these TCR-T cells with a small molecule inhibitor
473 of SPT6.

474 Our investigation into lysine methylation on $KRAS_{G12V}$ antigen revealed an intriguing role of
475 PTMs in changing recognition of tumor cells by cytotoxic T cells and provided a strategy to mitigate the
476 effects of PTMs to produce more consistently performing therapeutic TCRs. PTMs of tumor-associated
477 antigens have previously been implicated in altering immunogenicity of tumor cells in several tumor
478 types (*58*), and we build upon this by describing a strategy for the development of TCRs to specifically
479 target them. This strategy paves the way for developing TCRs that specifically target PTMs, offering a
480 novel avenue for personalized immunotherapy. Moreover, we have identified TCRs that can target and
481 kill tumor cells with mutated $KRAS_{G12V}$ and that are restricted to the most common human HLA allele,
482 which therefore has significant direct potential for clinical development. The widespread expression of
483 the $KRAS_{G12V}$ mutation across numerous different tumor types, including many solid tumors, means these
484 TCRs may allow for a substantially broadened therapeutic scope of ACT to combat these otherwise
485 difficult-to-treat tumors, including a wide variety of solid tumors.

486 The roles of PTMs found on tumor antigens outside of altering tumor cell immunogenicity are
487 likely broad. In the case of HLA-A2-presented $KRAS_{G12V}$, lysine-5 methylation in KRAS has been
488 speculated to affect interactions with relevant signaling proteins in the Ras family pathway signaling (*34*).

489 Characterizing the mechanistic reasons for and consequences of PTMs on tumor antigens should grant
490 additional insight into possible molecular pathways that could be targeted synergistically with, or
491 independently of, immunotherapies targeting these antigens.
492

493 Materials and Methods

494 Computational modeling of TCR:pMHC complexes.

495 We used Alphafold to generate an initial structural model comprising a given TCR and pMHC
496 complex with unmodified KRAS epitope. Using the resulting model of the TCR:pMHC complex not yet
497 including any PTMs, we used PyRosetta (*48*) 2023.49 to introduce relevant PTMs to the epitope, then
498 reoptimize the binding energy of the TCR:pMHC complex with the PTMs under consideration to create
499 the final structural model. Subsequent visualizations were generated using VMD (*59*). For modeling only
500 the pMHC complex, we used PyRosetta to take a pMHC complex with known structure, consisting of
501 HLA-A2 presenting a peptide with a sequence similar to $KRAS_{G12V}$ 5-14, LLFGYPVAV (PDB: 1QSF
502 (*60*)), mutated the peptide to $KRAS_{G12V}$ 5-14 with or without PTMs, and reoptimized the binding energy
503 of the resulting pMHC complex.
504

505 Generation and use of lentiviral constructs for TCRs.

506 We created lentiviral transfer plasmids expressing our TCRs, using pRRLSIN as a basis. We
507 digested this plasmid with AscI and PstI restriction enzymes (New England Biolabs), with recognition
508 sites being introduced at appropriate locations beforehand via site-directed mutagenesis, and gel-extracted
509 the backbone. We then performed Gibson assembly using the Gibson Assembly Kit (New England
510 Biolabs) on the digested backbone and synthesized DNA blocks (Codex DNA; Integrated DNA
511 Technologies) encoding codon-optimized versions of our selected TCR sequences. The Gibson assembly
512 products were transformed into chemically competent 5-alpha *E. coli* bacteria (New England Biolabs).
513 The final construct thus contained a single open reading frame for the TCR, composed of the TCRβ chain,

514 P2A, and TCRα chain and driven by the MSCV U3 promoter. To verify sequences of resulting clones, we
515 used the full plasmid sequencing service from Primordium Labs.
516 To generate lentivirus for TCR expression, we cultured 293T cells in RPMI 1640 media (Thermo
517 Fisher) with 5% FBS (Cytiva), 5% human serum (Bloodworks Northwest), 0.6% MEM Non-Essential
518 Amino Acids solution (Thermo Fisher), 4 mM L-glutamine (Gibco), and 100 U/ml penicillin-
519 streptomycin (Gibco). To generate lentivirus from the above constructs, we transfected the 293T cells at 3
520 million cells/10 cm dish with Effectene transfection reagent (Qiagen) following manufacturer guidelines,
521 using 1.5 μg of an individual TCR construct, 0.5 μg of pMD2.G (Addgene #12259), 1 μg of
522 pMDLg/pRRE (Addgene #12251), and 1 μg of pRSV-Rev (Addgene #12253). 1 d after transfection, we
523 changed media, removing transfection reagent; 1 d following that, we filtered culture supernatant through
524 0.45 μm PVDF filters. The filtered product was stored at –80ºC until used in TCR-T cell generation.
525
526 TCR-T cell generation.
527 We isolated $CD8^+$ T cells from primary human donor PBMCs using the EasySep Human $CD8^+$ T
528 cell Isolation Kit (STEMCELL Technologies) and activated them overnight using anti-CD3/CD28
529 DynaBeads (Thermo Fisher). Afterward, we transduced these T cells with lentivirus to express an
530 engineered TCR targeting HLA-A2-presented $KRAS_{G12V}$ epitope, including spinfection at 1,055 *g* for 90
531 minutes at 30°C. Cells were grown in "CTL media": RPMI 1640 media (Thermo Fisher) with 10%
532 human serum (Bloodworks Northwest), 4 mM L-glutamine (Gibco), 100 U/ml penicillin-streptomycin
533 (Gibco), and 50 IU/ml IL-2 (Prometheus; obtained via University of Washington Pharmacy, DOH license
534 #DRRS.FX.60550751), with medium changes every 2-3 d. Cells were sorted for peptide-MHC tetramer
535 binding 6 d after transduction. These cells were expanded via rapid expansion protocol for 8–14 d as
536 described previously(*61*). At the end of expansion, the cells were used for functional assays.
537
538 MS of KRAS protein and ARTEMIS.

539 We performed ARTEMIS following previously described procedure(*42*) on DAN-G human
540 pancreatic adenocarcinoma and 293F cell lines. Briefly, we transduced these cell lines with a construct
541 expressing secreted, His-tagged HLA-A2 single chain dimer (SCD) with mCherry and a construct for
542 constitutive expression of the first 100 amino acids of human $KRAS_{G12V}$, based on Lenti-mCherry-G12V-
543 KRAS-IRES-Blast (Addgene #153336). Cells were sorted for SCD expression via mCherry and further
544 selected for the truncated $KRAS_{G12V}$ expression via blasticidin at 10 µg/ml for 7 d. We expanded these
545 cells and harvested culture supernatant for two weeks. We filtered out debris from this supernatant using a
546 0.6 µm filter, captured HLA-A2 SCD-peptide complex with Ni-NTA agarose beads (Invitrogen) in
547 imidazole equilibration buffer (10mM imidazole, 300 mM NaCl, 50 mM NaH_2PO_4, pH 8), and eluted the
548 bound peptides in a denaturing buffer (5M guanidine-HCl, 250 mM NaCl, 50 mM NaH_2PO_4, 1 mM DTT,
549 pH 8).

550 For whole KRAS protein, we performed cell lysis on HLA-$A2^+$ tumor cell lines to collect protein
551 as described previously(*62*). From the resulting protein extract, we performed immunoprecipitation for
552 KRAS using MS-compatible magnetic immunoprecipitation kit (Pierce) and anti-KRAS antibody (12063-
553 1-AP; Thermo Fisher), following manufacturer guidelines. The immunoprecipitated protein was run
554 through SDS-PAGE, and a protein band at ~21 kDa size was excised and used for liquid chromatography-
555 MS.

556

557 <u>Discovery of new TCRs via mutagenesis of an existing TCR targeting HLA-A2-presented $KRAS_{G12V}$ 5-</u>
558 <u>14.</u>

559 To generate rationalized mutagenesis libraries of TCR_2 targeting the sequence within CDR3α as
560 selected from the structural prediction, we performed Gibson assembly to combine synthesized saturation
561 mutagenesis DNA blocks replacing the identified 'core' residues of CDR3α with the remainder of the
562 TCR_2 construct. We transduced these TCR libraries into populations of Jurkat cells expressing CD8 and
563 the Nur77-green fluorescent protein (GFP) reporter gene, which specifically permits measurement of
564 TCR signaling(*51*). These cells were grown in CTL media with the addition of $KRAS_{G12V}$ 5-14, with or

565 without methylation of the lysine-5 side chain, and presented by HLA-A2. After two weeks, we sorted
566 these cells for binding to tetramers of HLA-A2 with unmethylated or methylated $KRAS_{G12V}$ epitope and
567 amplified CDR3α sequences from sorted cells. Amplicons were sequenced by next-generation sequencing
568 on an Illumina MiSeq v2 flow cell with paired-end 150 bp reads.

569 To process sequencing results, we used custom code, trimming adapters and using Bowtie2 to
570 align reads to a reference sequence for the CDR3α region of TCR_2. We then scanned for variations from
571 the reference sequence and compared the frequencies of individual sequence variants between sorted
572 populations. The most differentially detected variants were cloned into new lentiviral TCR constructs
573 based on pRRLSIN, as described in the section "Generation and use of lentiviral constructs for TCRs".
574

575 <u>Discovery of new TCRs by stimulation of primary T cells by MHC I-presented peptides.</u>

576 To enrich T cells expressing TCRs from the centrally tolerated human TCR repertoire that could
577 recognize HLA-A2-presented $KRAS_{G12V}$ epitope, we isolated primary $CD8^+$ T cells from HLA-$A2^+$,
578 healthy human donor PBMCs (**Fig. S4a**). From the remaining PBMCs, we generated mature DCs through
579 a differentiation cocktail consisting of GM-CSF and IL-4 (Peprotech) for 1 d followed by TNFα, IL-1β,
580 IL-6 (Peprotech), and prostaglandin E2 (MP Biochemicals) for 1 d. The resulting DCs acted as APCs:
581 they were pulsed for 4 h with synthetic $KRAS_{G12V}$ peptides (Elim Biopharm), with or without PTMs
582 incorporated, and stimulated the $CD8^+$ T cells with the resulting peptide-presenting DCs. After this initial
583 stimulation, we continued to expand the T cells with a combination of IL-2 (Prometheus; obtained via
584 University of Washington Pharmacy, DOH license #DRRS.FX.60550751), IL-7, and IL-15 (Peprotech)
585 with medium replenishment every 2–3 d. These T cells were brought through multiple cycles of this
586 stimulation. In subsequent stimulations, peptide presentation was done by peptide-pulsing PBMCs instead
587 of mature DCs. At the end of the final round of stimulation, we stained T cells with HLA-A2 tetramers
588 presenting $KRAS_{G12V}$ 5-14 (with or without PTMs) and conjugated to a fluorophore, with a different
589 fluorophore per PTM/unmodified peptide. These cells were sorted into separate populations based on
590 tetramer binding patterns.

591 From the sorted T cells, we quantitated TCR clonotypes using the ImmunoSEQ assay (Adaptive
592 Biotech) and performed single cell RNA-seq using the Chromium Single Cell V(D)J Enrichment Kit for
593 T cells (10X Genomics) to identify paired TCRa/TCRb sequences. Using Cellranger 7.0.0 followed by
594 Loupe VDJ Browser 4.0, for each population, we selected the most highly enriched sequences for cloning
595 of TCR lentiviral constructs.
596
597 Coculture with engineered TCR-T cells and HLA-A2$^+$ tumor cells.
598 HLA-A2$^+$ tumor cell lines were lentivirally transduced to express either Nuclight-Red or
599 Nuclight-Green nuclear-localizing fluorescent protein (Sartorius) and sorted for their expression. For co-
600 culture with TCR-T cells, we plated the tumor cell lines on 48-well plates at a density of 10,000 cells/well
601 one day before adding T cells to allow for tumor cell adherence. T cells, generated as described above,
602 were added to these wells at a CD8$^+$ T cell:tumor cell ratio of 4:1 unless stated otherwise, with an initial
603 dose of 12.5 IU/ml IL-2. Cocultures were imaged every two hours at 10X magnification using an Incucyte
604 S3 machine (Sartorius).
605
606 *In vitro* peptide assays.
607 To determine functional avidity of our engineered TCRs against peptides, we used either Jurkat
608 CD8$^+$ Nur77-GFP reporter cells or primary human HLA-A2$^+$ T cells and transduced them with one of our
609 TCRs. Cells were incubated with *TAP*-deficient T2 cells and synthetic peptide at set concentrations, in the
610 presence of GolgiStop and GolgiPlug protein transport inhibitors (BD Biosciences) at 1:1000 dilution
611 each for 16 h at 37°C. Cells were incubated by themselves in the presence of the same protein transport
612 inhibitors in addition to synthetic peptides at set concentrations for 4 h at 37°C. At the end of incubation,
613 live CD8$^+$ cells were measured for expression of IFNγ (primary CD8$^+$ T cells) or Nur77-GFP (Jurkat
614 CD8$^+$ Nur77-GFP reporter cells) by flow cytometry. CD8$^+$ T cells were stained with eFluor 780 Fixable
615 Viability Dye (Invitrogen) followed by CD8:BV421 (Biolegend), fixed and permeabilized using the BD
616 Cytofix/Cytoperm Kit (BD Biosciences), and stained with IFNγ:PE-Cy7 antibody (Biolegend). Nur77-

617 GFP Jurkat cells were stained with CD8:BV421 (Biolegend) followed by propidium iodide. Flow
618 cytometry analysis was performed using FlowJo v9 (BD Biosciences).
619 To measure the stability of peptide presentation on HLA-A2, we incubated T2 cells with
620 individual peptides of interest for 16 h, then measured live cells for surface expression of HLA-A2 by
621 flow cytometry, staining with HLA-A2:FITC antibody (Biolegend) and propidium iodide.
622
623 CRISPR knockout screen and validation of genes involved in methylation processes.
624 Genes were selected using the PANTHER database (*63*) which met the criteria of containing
625 "methyl" in the gene ontology description. The total number of genes selected was 605. A total of 1,813
626 sgRNA sequences for the genes of interest were collected from existing databases (*64-66*). 30 control
627 gRNA sequences were added to the library for a total of 1,843 gRNAs (**Table S1**). The list of sgRNAs
628 was ordered as a custom oligonucleotide pool from Integrated DNA Technologies.

629 For the creation of the CRISPR knockout library plasmid, we performed cloning following
630 Canver *et al.*, 2018 (*67*). An oligo pool was cloned into lentiCRISPRv2 (Addgene #52961) which was
631 digested using Esp3I-HF (New England Biolabs). (2.5 µg) was transfected into HEK293T cells using X-
632 tremeGENE™ 9 (Roche) with psPAX2 (1.625 µg) and pCMV-VSV-G (0.875 µg) plasmids (Addgene
633 #12260, #8454). Viral supernatant was collected and filtered using a 0.45 µm PVDF filter 48 hours after
634 transfection. The plasmid-containing viral supernatant was then transduced into the DAN-G cell line. To
635 select for the cells which were successfully transduced, the cells underwent puromycin selection for 7
636 days at 1 µg/ml concentration with medium changes every 2-3 days. The library-containing DAN-G cells
637 were co-cultured with the KRAS-targeting TCR-T cells for 7 days. Following co-culture, the DAN-G
638 cells were rinsed with PBS and pelleted for genomic DNA extraction using QIAGEN DNeasy Blood &
639 Tissue kit. The sgRNA region of the genomic DNA was PCR amplified following the
640 'sgRNA/shRNA/ORF PCR for Illumina Sequencing' protocol via the Broad Institute Genetic
641 Perturbation Platform and assessed for fragment length distribution on TapeStation D1000 (Agilent).

642 Upon verification of fragment length, the samples were pooled and sequenced on an Illumina MiSeq
643 machine.
644 Raw NGS reads were adapter-trimmed with Cutadapt v2.9, followed by alignment to the
645 reference library with Bowtie v1.3. Comparisons between different conditions were performed using the
646 MAGeCK pipeline, using RRA and MLE algorithms for calculating statistical significance of results.
647 MAGeCK also predicts gene essentiality by evaluating the ranked list of sgRNAs (*68*).
648 To verify hits from our CRISPR library screen, we transduced DAN-G cells with lentivirus
649 inducing single knockouts and puromycin resistance. After 7 days of puromycin selection at 1 μg/ml, the
650 DAN-G single knockout cells was co-cultured with TCR-T cells at a 4:1 T cell:tumor cell ratio and
651 imaged every 4 hours at 10X magnification using an Incucyte S3 machine (Sartorius).
652 To verify knockout, genomic DNA was extracted from single knockout DAN-G cells, and the
653 gRNA region was PCR amplified using Q5 High-Fidelity DNA Polymerase (New England Biolabs),
654 yielding amplicon lengths of between 500-800 base pairs. The PCR-amplified samples were sequenced
655 using the "Premium PCR Sequencing" service from Primordium Labs. The resulting sequence files were
656 aligned with the reference genome using BWA-MEM to screen for the common mutation sites to confirm
657 the knockout. To verify the methylation status of HLA-A2-presented $KRAS_{G12V}$ epitope in the *SUPT6H*
658 knockout DAN-G cells and non-knocked-out DAN-G cells, we expanded these cells and extracted HLA-
659 A2-presented peptide using the ARTEMIS protocol as previously described.
660 To compare HLA-A2 expression of *SUPT6H* knockout vs. non-knocked-out cells, the cells were
661 stained with HLA-A2:PE antibody (Biolegend) and propidium iodide and analyzed via flow cytometry.
662 To compare KRAS expression, protein lysate was extracted from tumor cell lines as described above and
663 used as input for Western blots with anti-KRAS antibody (12063-1-AP; Thermo Fisher).
664
665
666

667 # References

668 1. T. M. Schmitt *et al.*, Generation of higher affinity T cell receptors by antigen-driven
669 differentiation of progenitor T cells in vitro. *Nat Biotechnol* **35**, 1188-1195 (2017).
670 2. A. G. Chapuis *et al.*, Transferred WT1-reactive CD8+ T cells can mediate antileukemic activity
671 and persist in post-transplant patients. *Sci Transl Med* **5**, 174ra127 (2013).
672 3. A. G. Chapuis *et al.*, T cell receptor gene therapy targeting WT1 prevents acute myeloid leukemia
673 relapse post-transplant. *Nat Med* **25**, 1064-1072 (2019).
674 4. D. Lu *et al.*, KRAS G12V neoantigen specific T cell receptor for adoptive T cell therapy against
675 tumors. *Nat Commun* **14**, 6389 (2023).
676 5. S. L. Doran *et al.*, T-Cell Receptor Gene Therapy for Human Papillomavirus-Associated
677 Epithelial Cancers: A First-in-Human, Phase I/II Study. *J Clin Oncol* **37**, 2759-2768 (2019).
678 6. I. A. Prior, F. E. Hood, J. L. Hartley, The Frequency of Ras Mutations in Cancer. *Cancer Res* **80**,
679 2969-2974 (2020).
680 7. G. A. Hobbs, C. J. Der, K. L. Rossman, RAS isoforms and mutations in cancer at a glance. *J Cell*
681 *Sci* **129**, 1287-1292 (2016).
682 8. J. H. Cook, G. E. M. Melloni, D. C. Gulhan, P. J. Park, K. M. Haigis, The origins and genetic
683 interactions of KRAS mutations are allele- and tissue-specific. *Nat Commun* **12**, 1808 (2021).
684 9. C. M. Rive *et al.*, Recombinant T cell receptors specific for HLA-A*02:01-restricted neoepitopes
685 containing KRAS codon 12 hotspot mutations. *bioRxiv*, 2020.2006.2015.149021 (2020).
686 10. E. Arrieta-Bolanos, D. I. Hernandez-Zaragoza, R. Barquera, An HLA map of the world: A
687 comparison of HLA frequencies in 200 worldwide populations reveals diverse patterns for class I
688 and class II. *Front Genet* **14**, 866407 (2023).
689 11. L. Chin *et al.*, Essential role for oncogenic Ras in tumour maintenance. *Nature* **400**, 468-472
690 (1999).

691 12. M. M. Awad *et al.*, Acquired Resistance to KRAS(G12C) Inhibition in Cancer. *N Engl J Med*
692 **384**, 2382-2393 (2021).
693 13. N. Tanaka *et al.*, Clinical Acquired Resistance to KRAS(G12C) Inhibition through a Novel
694 KRAS Switch-II Pocket Mutation and Polyclonal Alterations Converging on RAS-MAPK
695 Reactivation. *Cancer Discov* **11**, 1913-1922 (2021).
696 14. P. A. Janne *et al.*, Adagrasib in Non-Small-Cell Lung Cancer Harboring a KRAS(G12C)
697 Mutation. *N Engl J Med* **387**, 120-131 (2022).
698 15. G. K. Dy *et al.*, Long-Term Outcomes and Molecular Correlates of Sotorasib Efficacy in Patients
699 With Pretreated KRAS G12C-Mutated Non-Small-Cell Lung Cancer: 2-Year Analysis of
700 CodeBreaK 100. *J Clin Oncol* **41**, 3311-3317 (2023).
701 16. K.-i. H. Malcolm J. W. Sim, Zachary Stotz, Zhiya Yu, Jinghua Lu, Paul Brennan, Max Quastel,
702 Geraldine M. Gillespie, Eric O. Long, James C. Yang, Peter D. Sun. (BiorRxiv, 2024).
703 17. M. Zhang *et al.*, Identification and affinity enhancement of T-cell receptor targeting a
704 KRAS(G12V) cancer neoantigen. *Commun Biol* **7**, 512 (2024).
705 18. R. Leidner *et al.*, Neoantigen T-Cell Receptor Gene Therapy in Pancreatic Cancer. *N Engl J Med*
706 **386**, 2112-2119 (2022).
707 19. A. Poole *et al.*, Therapeutic high affinity T cell receptor targeting a KRAS(G12D) cancer
708 neoantigen. *Nat Commun* **13**, 5333 (2022).
709 20. F. F. Gonzalez-Galarza, S. Christmas, D. Middleton, A. R. Jones, Allele frequency net: a database
710 and online repository for immune gene frequencies in worldwide populations. *Nucleic Acids Res*
711 **39**, D913-919 (2011).
712 21. J. M. Ellis *et al.*, Frequencies of HLA-A2 alleles in five U.S. population groups. Predominance
713 Of A*02011 and identification of HLA-A*0231. *Hum Immunol* **61**, 334-340 (2000).
714 22. A. S. Bear *et al.*, Biochemical and functional characterization of mutant KRAS epitopes validates
715 this oncoprotein for immunological targeting. *Nat Commun* **12**, 4365 (2021).

716 23. J. Choi *et al.*, Systematic discovery and validation of T cell targets directed against oncogenic
717 KRAS mutations. *Cell Rep Methods* **1**, 100084 (2021).
718 24. M. Mishto *et al.*, An in silico-in vitro Pipeline Identifying an HLA-A(*)02:01(+) KRAS G12V(+)
719 Spliced Epitope Candidate for a Broad Tumor-Immune Response in Cancer Patients. *Front*
720 *Immunol* **10**, 2572 (2019).
721 25. M. C. Lahman *et al.*, Targeting an alternate Wilms' tumor antigen 1 peptide bypasses
722 immunoproteasome dependency. *Sci Transl Med* **14**, eabg8070 (2022).
723 26. A. K. Johnsen, D. J. Templeton, M. Sy, C. V. Harding, Deficiency of transporter for antigen
724 presentation (TAP) in tumor cells allows evasion of immune surveillance and increases
725 tumorigenesis. *J Immunol* **163**, 4224-4231 (1999).
726 27. L. Maggs, A. Sadagopan, A. S. Moghaddam, S. Ferrone, HLA class I antigen processing
727 machinery defects in antitumor immunity and immunotherapy. *Trends Cancer* **7**, 1089-1101
728 (2021).
729 28. L. L. Hardy, D. A. Wick, J. R. Webb, Conversion of tyrosine to the inflammation-associated
730 analog 3'-nitrotyrosine at either TCR- or MHC-contact positions can profoundly affect
731 recognition of the MHC class I-restricted epitope of lymphocytic choriomeningitis virus
732 glycoprotein 33 by CD8 T cells. *J Immunol* **180**, 5956-5962 (2008).
733 29. V. Corbiere *et al.*, Natural T Cell Epitope Containing Methyl Lysines on Mycobacterial Heparin-
734 Binding Hemagglutinin. *J Immunol* **204**, 1715-1723 (2020).
735 30. J. Petersen *et al.*, Phosphorylated self-peptides alter human leukocyte antigen class I-restricted
736 antigen presentation and generate tumor-specific epitopes. *Proc Natl Acad Sci U S A* **106**, 2776-
737 2781 (2009).
738 31. B. Raposo *et al.*, T cells specific for post-translational modifications escape intrathymic tolerance
739 induction. *Nat Commun* **9**, 353 (2018).
740 32. P. K. Mazur *et al.*, SMYD3 links lysine methylation of MAP3K2 to Ras-driven cancer. *Nature*
741 **510**, 283-287 (2014).

742 33. C. Y. Chiang *et al.*, Methylation of KRAS by SETD7 promotes KRAS degradation in non-small
743 cell lung cancer. *Cell Rep* **42**, 113003 (2023).
744 34. H. Yoshino *et al.*, Identification of lysine methylation in the core GTPase domain by
745 GoMADScan. *PLoS One* **14**, e0219436 (2019).
746 35. E. Caron *et al.*, Analysis of Major Histocompatibility Complex (MHC) Immunopeptidomes
747 Using Mass Spectrometry. *Mol Cell Proteomics* **14**, 3105-3117 (2015).
748 36. C. Hughes, B. Ma, G. A. Lajoie, De novo sequencing methods in proteomics. *Methods Mol Biol*
749 **604**, 105-121 (2010).
750 37. I. Perdivara, L. J. Deterding, M. Przybylski, K. B. Tomer, Mass spectrometric identification of
751 oxidative modifications of tryptophan residues in proteins: chemical artifact or post-translational
752 modification? *J Am Soc Mass Spectrom* **21**, 1114-1117 (2010).
753 38. B. Peters, M. Nielsen, A. Sette, T Cell Epitope Predictions. *Annu Rev Immunol* **38**, 123-145
754 (2020).
755 39. I. Ahearn, M. Zhou, M. R. Philips, Posttranslational Modifications of RAS Proteins. *Cold Spring*
756 *Harb Perspect Med* **8**, (2018).
757 40. C. L. W. Miller, J. L. Warner, F. Winston, Insights into Spt6: a histone chaperone that functions
758 in transcription, DNA replication, and genome stability. *Trends Genet* **39**, 858-872 (2023).
759 41. B. Reynisson, B. Alvarez, S. Paul, B. Peters, M. Nielsen, NetMHCpan-4.1 and NetMHCIIpan-
760 4.0: improved predictions of MHC antigen presentation by concurrent motif deconvolution and
761 integration of MS MHC eluted ligand data. *Nucleic Acids Res* **48**, W449-W454 (2020).
762 42. K. A. K. Finton *et al.*, ARTEMIS: A Novel Mass-Spec Platform for HLA-Restricted Self and
763 Disease-Associated Peptide Discovery. *Front Immunol* **12**, 658372 (2021).
764 43. A. Ooi, A. Wong, L. Esau, F. Lemtiri-Chlieh, C. Gehring, A Guide to Transient Expression of
765 Membrane Proteins in HEK-293 Cells for Functional Characterization. *Front Physiol* **7**, 300
766 (2016).

767 44. B. Y. Tew *et al.*, Genome-wide DNA methylation analysis of KRAS mutant cell lines. *Sci Rep*
768 **10**, 10149 (2020).
769 45. H. Jin *et al.*, Epigenetic silencing of a Ca(2+)-regulated Ras GTPase-activating protein RASAL
770 defines a new mechanism of Ras activation in human cancers. *Proc Natl Acad Sci U S A* **104**,
771 12353-12358 (2007).
772 46. M. Chen *et al.*, Tryptic Peptides Bearing C-Terminal Dimethyllysine Need to Be Considered
773 during the Analysis of Lysine Dimethylation in Proteomic Study. *J Proteome Res* **16**, 3460-3469
774 (2017).
775 47. H. W. Nijman *et al.*, Identification of peptide sequences that potentially trigger HLA-A2.1-
776 restricted cytotoxic T lymphocytes. *Eur J Immunol* **23**, 1215-1219 (1993).
777 48. S. Chaudhury, S. Lyskov, J. J. Gray, PyRosetta: a script-based interface for implementing
778 molecular modeling algorithms using Rosetta. *Bioinformatics* **26**, 689-691 (2010).
779 49. A. R. Karapetyan *et al.*, TCR Fingerprinting and Off-Target Peptide Identification. *Front*
780 *Immunol* **10**, 2501 (2019).
781 50. J. Jumper *et al.*, Highly accurate protein structure prediction with AlphaFold. *Nature* **596**, 583-
782 589 (2021).
783 51. J. F. Ashouri, A. Weiss, Endogenous Nur77 Is a Specific Indicator of Antigen Receptor Signaling
784 in Human T and B Cells. *J Immunol* **198**, 657-668 (2017).
785 52. D. Hudson, R. A. Fernandes, M. Basham, G. Ogg, H. Koohy, Can we predict T cell specificity
786 with digital biology and machine learning? *Nat Rev Immunol* **23**, 511-521 (2023).
787 53. P. Bradley, Structure-based prediction of T cell receptor:peptide-MHC interactions. *Elife* **12**,
788 (2023).
789 54. P. Moris *et al.*, Current challenges for unseen-epitope TCR interaction prediction and a new
790 perspective derived from image classification. *Brief Bioinform* **22**, (2021).
791 55. H. Bagdonas, C. A. Fogarty, E. Fadda, J. Agirre, The case for post-predictional modifications in
792 the AlphaFold Protein Structure Database. *Nat Struct Mol Biol* **28**, 869-870 (2021).

793 56. P. D. Renfrew, E. J. Choi, R. Bonneau, B. Kuhlman, Incorporation of noncanonical amino acids
794 into Rosetta and use in computational protein-peptide interface design. *PLoS One* **7**, e32637
795 (2012).
796 57. J. Liu, Q. Wang, Y. Kang, S. Xu, D. Pang, Unconventional protein post-translational
797 modifications: the helmsmen in breast cancer. *Cell Biosci* **12**, 22 (2022).
798 58. A. K. Srivastava, G. Guadagnin, P. Cappello, F. Novelli, Post-Translational Modifications in
799 Tumor-Associated Antigens as a Platform for Novel Immuno-Oncology Therapies. *Cancers*
800 *(Basel)* **15**, (2022).
801 59. W. Humphrey, A. Dalke, K. Schulten, VMD: visual molecular dynamics. *J Mol Graph* **14**, 33-38,
802 27-38 (1996).
803 60. Y. H. Ding, B. M. Baker, D. N. Garboczi, W. E. Biddison, D. C. Wiley, Four A6-
804 TCR/peptide/HLA-A2 structures that generate very different T cell signals are nearly identical.
805 *Immunity* **11**, 45-56 (1999).
806 61. S. R. Riddell, P. D. Greenberg. (Google Patents, 2000).
807 62. L. M. Adams, C. J. DeHart, N. L. Kelleher, Precise Characterization of KRAS4B Proteoforms by
808 Combining Immunoprecipitation with Top-Down Mass Spectrometry. *Methods Mol Biol* **2262**,
809 47-64 (2021).
810 63. H. Mi *et al.*, PANTHER version 16: a revised family classification, tree-based classification tool,
811 enhancer regions and extensive API. *Nucleic Acids Res* **49**, D394-D403 (2021).
812 64. N. E. Sanjana, O. Shalem, F. Zhang, Improved vectors and genome-wide libraries for CRISPR
813 screening. *Nat Methods* **11**, 783-784 (2014).
814 65. J. G. Doench *et al.*, Optimized sgRNA design to maximize activity and minimize off-target
815 effects of CRISPR-Cas9. *Nat Biotechnol* **34**, 184-191 (2016).
816 66. J. P. Concordet, M. Haeussler, CRISPOR: intuitive guide selection for CRISPR/Cas9 genome
817 editing experiments and screens. *Nucleic Acids Res* **46**, W242-W245 (2018).

67. M. C. Canver *et al.*, Integrated design, execution, and analysis of arrayed and pooled CRISPR genome-editing experiments. *Nat Protoc* **13**, 946-986 (2018).

68. W. Li *et al.*, MAGeCK enables robust identification of essential genes from genome-scale CRISPR/Cas9 knockout screens. *Genome Biol* **15**, 554 (2014).

Acknowledgements

We would like to thank the Fred Hutch Genomics, Bioinformatics, Proteomics/Metabolomics, Flow Cytometry, and Cellular Imaging Shared Resources for their respective roles in helping to run key experiments. We also thank members of the Chapuis Lab and the Strong Lab at Fred Hutch for their help setting up ARTEMIS for use in this study.

Funding: This study received financial support from donations to Fred Hutchinson Cancer Center for "TCR Therapy for Patients with Pancreatic Cancers" (Fred Hutch Reference Number SRA210802) and Affini-T Therapeutics, Inc. (Fred Hutch Reference Number 20012884). The mass spectrometry instrumentation used in this research was funded by a grant from the National Institutes of Health Office of Research Infrastructure Programs (grant S10OD030225). Fred Hutch Shared Resources were supported by the Fred Hutch/University of Washington/Seattle Children's Cancer Consortium Cancer Center Support Grant (National Institutes of Health grant P30CA015704).

Author contributions:

Conceptualization: JWL, RP, TM, PB, AGC, TMS, PDG

Methodology: JWL, EYC, RP, MEC, TM, YS, PB, TMS, PDG

Investigation: JWL, EYC, TH, RP, MEC, TM, SM, CLM, LNJ, PRG, PC, PB, TMS

Visualization: JWL, EYC, TMS

Funding acquisition: RP, TM, AGC, PB, TMS, PDG

Project administration: AGC, TMS, PDG

Supervision: PB, TMS, PDG

Writing – original draft: JWL, EYC

Writing – review & editing: JWL, EYC, TH, RP, MEC, TM, LNJ, PRG, PC, YS, AGC, TMS, PDG

Competing interests: PDG is on the Scientific Advisory Board of Celsius, Earli, Elpiscience, Immunoscape, Rapt, Catalio, and Nextech, was a scientific founder of Juno Therapeutics, and receives research support from Lonza. RP, TM, AGC, TMS, and PDG are co-inventors on a patent associated with technology described in this work that is licensed to Affini-T. AGC, TMS, and PDG are co-founders of, have equity in, and receive research support from Affini-T. All other authors declare that they have no competing interests.

Data and materials availability: Code for structural modeling and TCR sequence data processing from TCR mutagenesis are available at https://github.com/jihoonlee0/A2_KRAS-G12V.

Figures and Tables

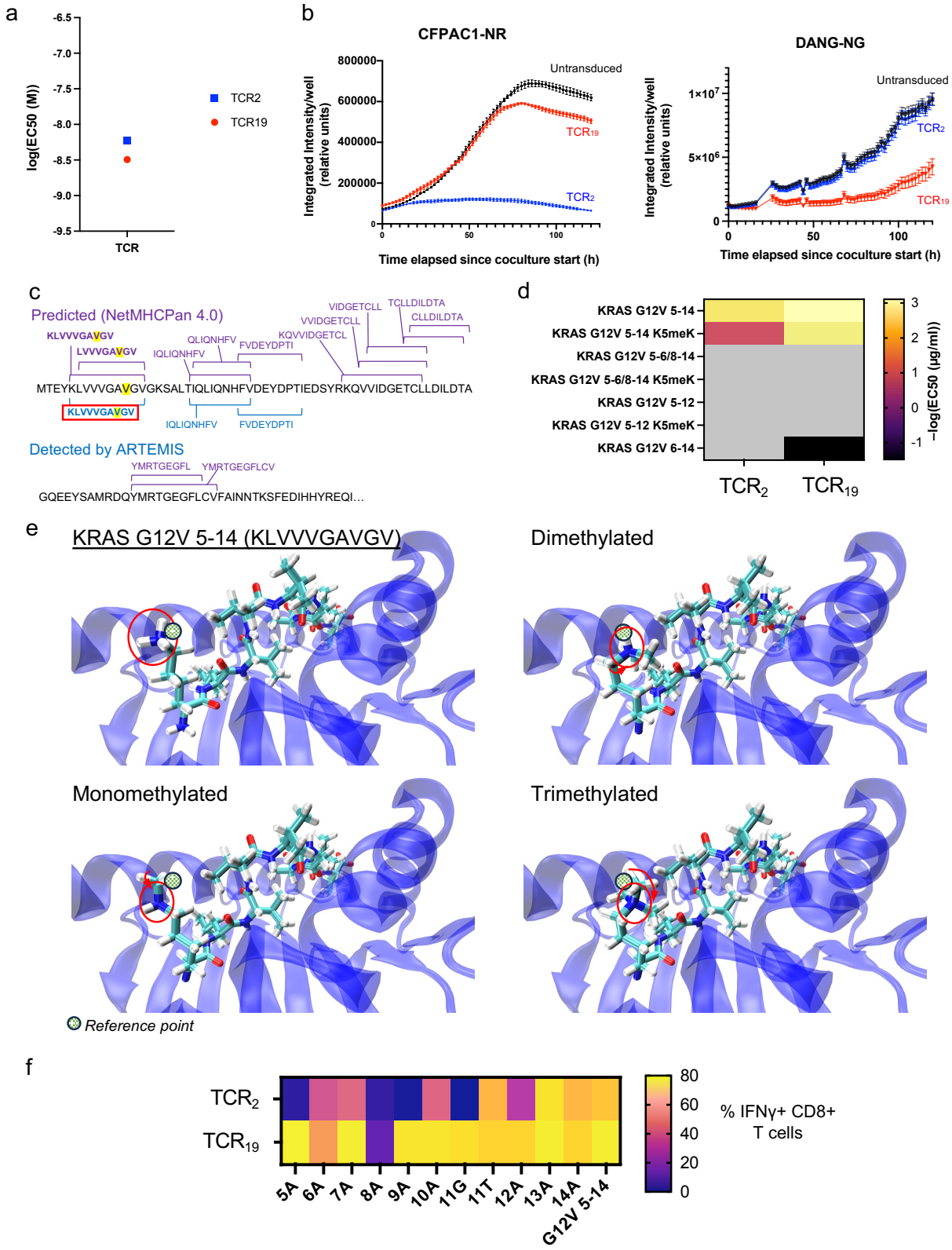

839 **Fig. 1:** Posttranslational modification on the HLA-A2-presented $KRAS_{G12V}$ epitope alters recognition of
840 the antigen by MHC class I-restricted TCRs and subsequent tumor cell killing. (a) $Log_{10}(EC_{50}$ (M))
841 comparison of recognition of different concentrations of a synthetic $KRAS_{G12V}$ 5-14 peptide
842 (KLVVVGAVGV) presented by HLA-A2 by different MHC class I-restricted TCRs specific for the
843 epitope. Lower values indicate higher functional avidity. (b) Killing of live CFPAC1 and DAN-G HLA-
844 $A2^+$ $KRAS_{G12V}^+$ pancreatic adenocarcinoma cells cocultured with $CD8^+$ T cells expressing the TCRs
845 shown in (a) using a 4:1 T cell:tumor cell ratio. Cocultures were recorded by Incucyte imaging. Tumor
846 cells expressed nuclear fluorescent protein; NR: red fluorescent protein; NG: green fluorescent protein.
847 (c) ARTEMIS MS data of peptides eluted from HLA-A2. Data is from the 293F cell line, as commonly
848 used for proteomics assays requiring high protein expression. All cell lines were transduced with an HLA-
849 A2 single chain secreted dimer as well as a $KRAS_{G12V}$ constitutive expression construct to increase
850 presentation and the likelihood of detecting a presented peptide by MS, of $KRAS_{G12V}$-related epitopes.
851 The first 100 amino acids of $KRAS_{G12V}$ are shown, with the G12V mutation highlighted in yellow.
852 Epitopes predicted by NetMHCPan 4.1 are shown in purple; epitopes detected from ARTEMIS are shown
853 in blue. ARTEMIS detection of $KRAS_{G12V}$ 5-14 is outlined in red. (d) Heatmap of $-log_{10}(EC_{50}$ (μg/ml)) of
854 $CD8^+$ T cells expressing TCR_2 or TCR_{19} against candidate $KRAS_{G12V}$ epitopes, with and without
855 methylation of the lysine-5 side chain of the epitope, presented by HLA-A2. Higher values indicate
856 higher functional avidity. EC_{50} values were calculated from T cell exposure to peptide concentrations
857 ranging from 1 μg/ml to 10^{-5} μg/ml. Gray squares indicate EC_{50} calculations that lacked a stable fit, e.g.,
858 due to lack of response to peptide even at high doses. (e) Rosetta structural modeling of HLA-A2
859 presenting $KRAS_{G12V}$ 5-14 and its methylated variants. Red circles indicate the amine group of the lysine-
860 5 side chain; arrows indicate its movement with different methylation states. A reference point is drawn at
861 the same position in each image to help illustrate positional changes. (f) Alanine scan of the $KRAS_{G12V}$
862 epitope and resulting response by $CD8^+$ T cells expressing TCR_2 and TCR_{19}. The epitope with each
863 individual residue substituted with alanine (or, for alanine-11, substituted with either glycine or threonine)
864 was presented by antigen-presenting cells to stimulate primary human $CD8^+$ T cells expressing a TCR,

and subsequent IFNγ expression was measured. Higher IFNγ induction indicates greater tolerance for amino acid substitution at that position. X-axis numbers indicate the residue number on the KRAS protein, and letters indicate the amino acid substitution. A: alanine; G: glycine; T: threonine. Last column is unmodified $KRAS_{G12V}$ 5-14.

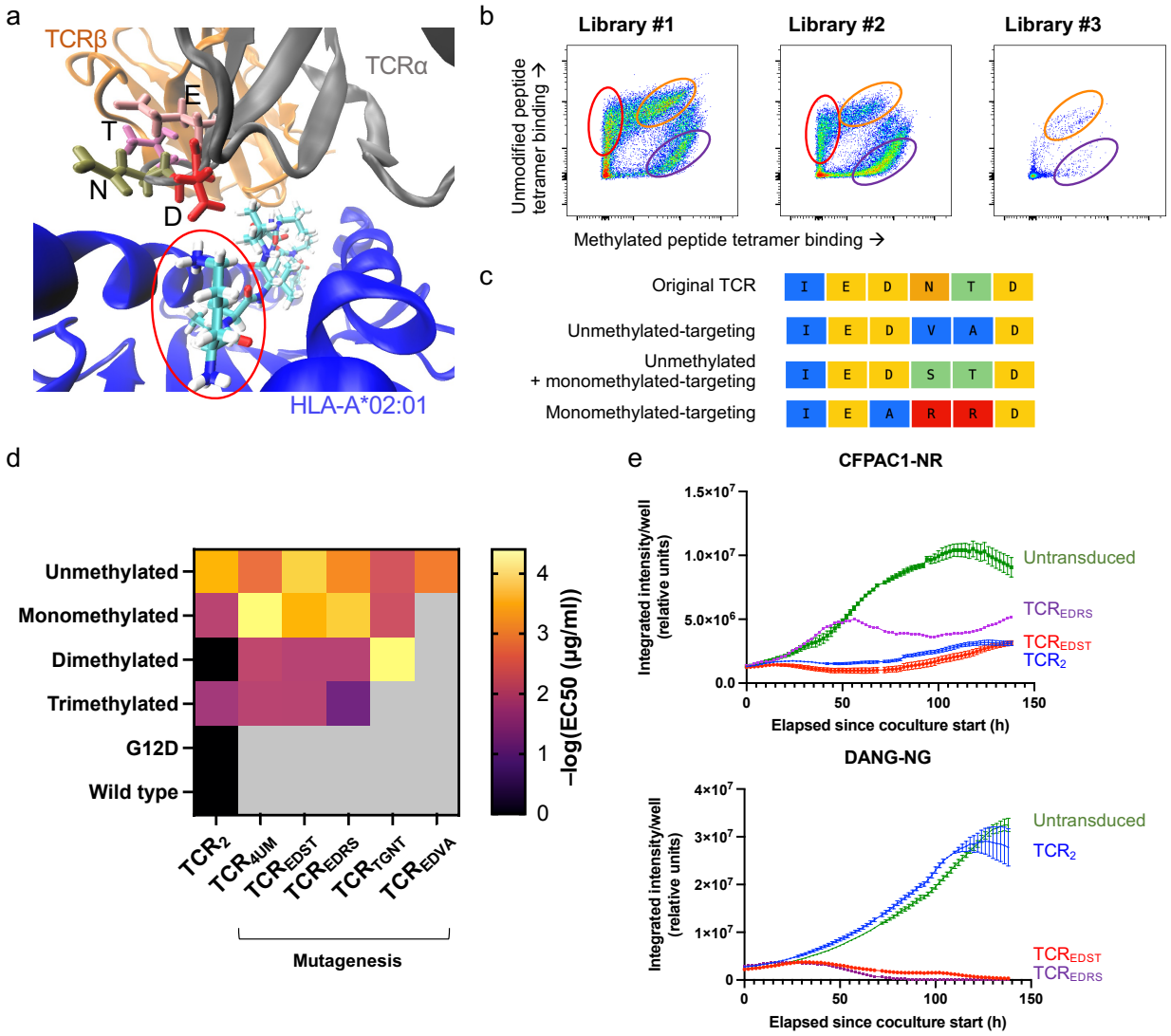

Fig. 2: A computationally guided, rationalized mutagenesis library to develop MHC class I-restricted TCRs that recognize methylated epitopes of HLA-A2-presented $KRAS_{G12V}$ and achieve enhanced targeting of HLA-A2$^+$ $KRAS_{G12V}^+$ tumor cell lines. (a) Structural model, as predicted by a combined Alphafold-Rosetta pipeline, of a 'core' CDR3α sequence (sequence EDNT) of an existing TCR

875 recognizing $KRAS_{G12V}$ 5-14 and its relation to the lysine-5 side chain (circled in red) of the epitope as
876 presented by HLA-A2. (b) Generation of TCR mutagenesis libraries by mutagenesis of the core CDR3α
877 sequence followed by transduction of the TCRs into Nur77-GFP reporter Jurkat cells and subsequent
878 clonal expansions. Tetramer binding patterns of HLA-A2-$KRAS_{G12V}$ 5-14 peptide with unmodified or
879 methylated lysine-5 side chain at the end of cell stimulation are shown. Each circle indicates a population
880 with a specific pattern of unmethylated vs. methylated peptide tetramer binding that was sorted and
881 sequenced. (c) Examples of mutated CDR3α 'core' sequences resulting from sorted clones of the
882 mutagenesis library that exhibit the noted different patterns of PTM peptide recognition. (d) Heatmap of –
883 $\log_{10}(EC_{50}$ (μg/ml)) of TCRs derived from the mutagenesis library and the original TCR_2 responding to
884 different degrees of lysine-5 methylation of $KRAS_{G12V}$ 5-14 presented by HLA-A2, as calculated from
885 dose response assays. Gray squares indicate EC_{50} values that lacked a stable fit, e.g., due to limited
886 response to peptide even at high doses. TCR_{4UM} is the 4th TCR clonotype identified from an initial
887 sequencing dataset from sorted Jurkat cells binding to both unmethylated ("U") and methylated ("M")
888 tetramers; other TCRs are labeled by changes in the 'core' CDR3α sequence (e.g., EDST). (e) Killing of
889 HLA-$A2^+$ $KRAS_{G12V}{}^+$ CFPAC1 and DAN-G pancreatic adenocarcinoma cells by $CD8^+$ T cells expressing
890 selected mutagenized TCRs. Cocultures of T cells and tumor cells were recorded by Incucyte imaging.
891 Tumor cells expressed nuclear fluorescent protein. NR: red fluorescent protein; NG: green fluorescent
892 protein.
893

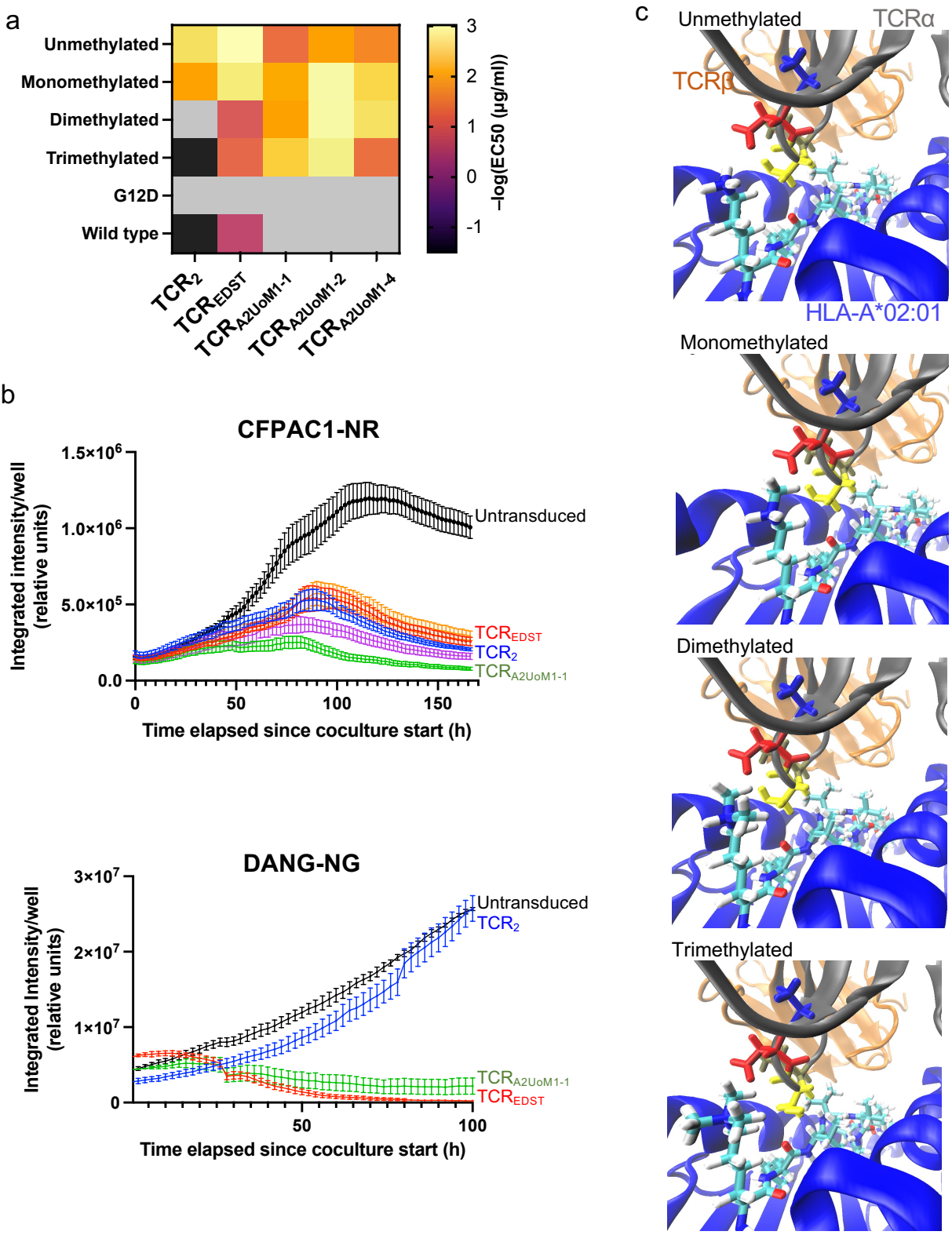

894

895 **Fig. 3:** Stimulation of primary human T cells with unmethylated and methylated HLA-A2-presented

896 $KRAS_{G12V}$ to generate MHC class I-restricted TCRs from a normal repertoire that recognize methylated

897 epitopes. (a) Heatmap of $-\log_{10}(EC_{50}$ (μg/ml)) of selected TCRs responding to the unmethylated and
898 methylated epitopes presented by HLA-A2, as calculated from dose response assays. Higher values
899 indicate higher functional avidity. Gray squares indicate EC_{50} values that lacked a stable fit, e.g., due to
900 limited response to peptide even at high doses. (b) Killing of HLA-A2$^+$ KRAS$_{G12V}^+$ CFPAC1 and DAN-G
901 pancreatic adenocarcinoma cells by CD8$^+$ T cells expressing selected TCRs. Cocultures of fluorescently
902 labeled tumor cells and TCR-T cells were recorded by Incucyte imaging. Tumor cells expressed nuclear
903 fluorescent protein; NR: red fluorescent protein; NG: green fluorescent protein. (c) Alphafold-Rosetta
904 visualizations of TCR:pMHC complexes for TCR$_{A2UoM1-1}$, isolated from expansion of responding primary
905 human CD8$^+$ T cells from normal repertoires. Structures were generated for unmethylated and
906 mono/di/trimethylated versions of the epitope, presented by HLA-A2. The four CDR3α amino acids in
907 closest proximity to the lysine-5 side chain of KRAS$_{G12V}$ are shown with individual molecular bonds.
908

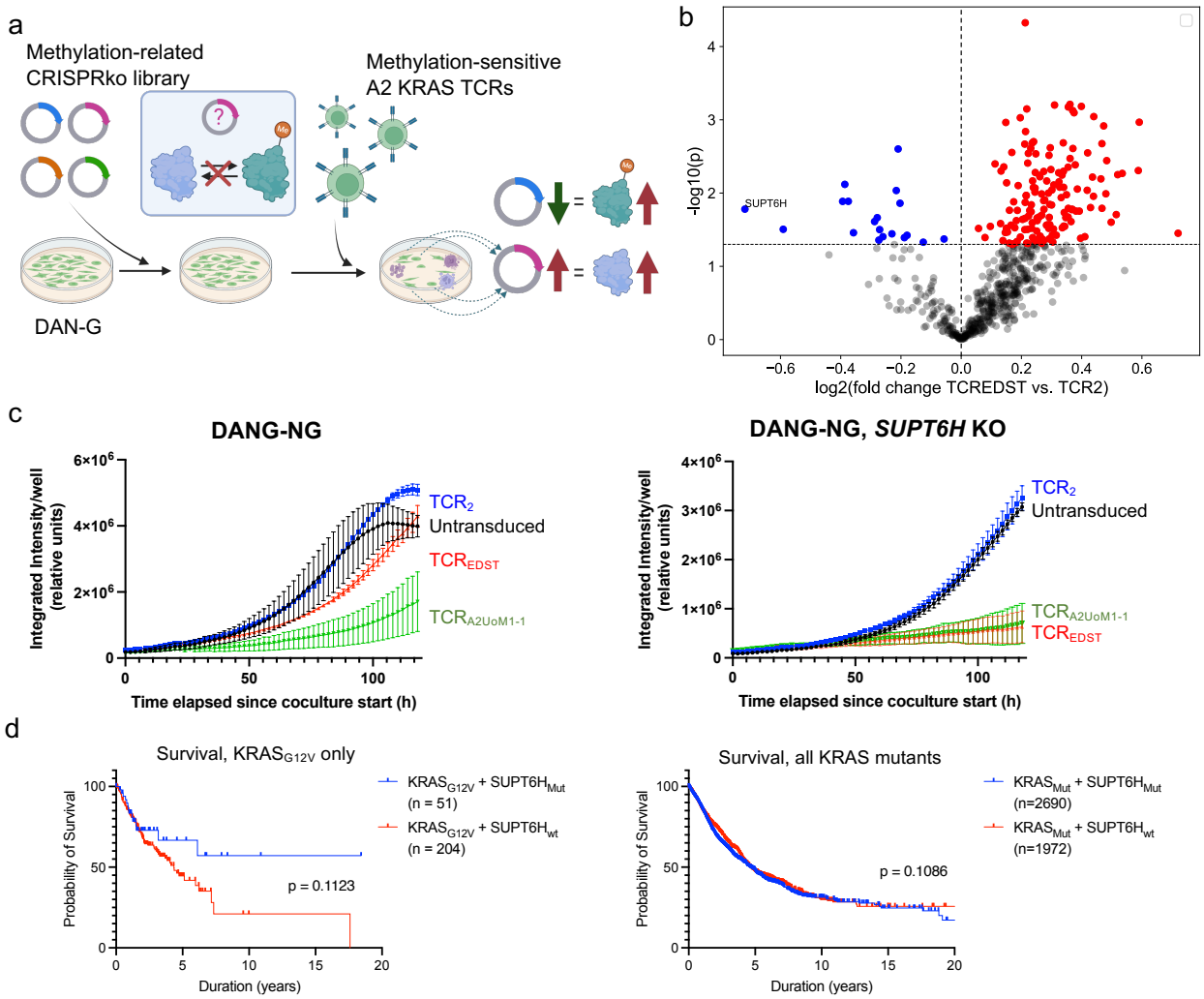

Fig. 4: A gene knockout screen for methylation-related genes identifies SPT6 (*SUPT6H*) as a participant in the demethylation of the HLA-A2-presented $KRAS_{G12V}$ epitope. (a) Overall workflow: DAN-G pancreatic adenocarcinoma cells were transduced with a CRISPR knockout library targeting methylation-related genes, and then cocultured with $CD8^+$ T cells expressing either TCR_2 or mutagenized TCR_{EDST}, which respectively have weak or strong recognition of methylated $KRAS_{G12V}$ epitopes. Tumor cells surviving at the end of coculture were sequenced to identify gRNA enrichment or depletion associated with immune evasion. (b) Volcano plot summarizing $\log_2$(fold change) of gRNA read frequencies targeting individual genes recovered after coculture of DAN-G cells with T cells expressing TCR_{EDST} versus TCR_2. The threshold of significance was set at $\log_{10}(p) < 1.2$ ($p < 0.05$) and is denoted by the horizontal dashed line. Mean counts of all gRNAs per gene were used to calculate fold change values.

920 The data point for gRNAs targeting *SUPT6H* is specifically labeled. The knockouts depleted or enriched
921 after cocultures using TCR_{EDST} versus TCR_2 are colored blue and red, respectively. (c) Killing of DAN-G
922 cells with or without *SUPT6H* knockout in coculture with selected TCR-T cells (untransduced or
923 expressing TCR_2, TCR_{EDST}, or $TCR_{A2UoM1-1}$). Cocultures of T cells and tumor cells were recorded by
924 Incucyte imaging. Tumor cells expressed green nuclear fluorescent protein ("NG"). (d) Kaplan-Meier
925 survival plots for individuals who have tumors with KRAS mutations, using public TCGA data. Left:
926 only tumors with the $KRAS_{G12V}$ mutant, with or without concurrent *SUPT6H* mutation. Right: tumors
927 with any KRAS mutant, with or without a concurrent *SUPT6H* mutation.
928

929 # Supplementary materials

930 Fig. S1 to S5
931 Table S1

a

Peptide sequence	Residues	%ile rank of HLA-A2 binding vs. random peptides
IQLIQNHFV	21-29	1.0784
KLVVVGAVGV	5-14	2.8794
LVVVGAVGV	6-14	3.1117
QLIQNHFV	22-29	3.8599
MTEYKLVVV	1-9	5.3608
GVGKSALTI	13-21	5.6588
TIQLIQNHFV	20-29	5.9529
GVGKSALTIQL	13-23	6.9975
KSALTIQLI	16-24	7.1313
KLVVVGAV	5-12	7.6549

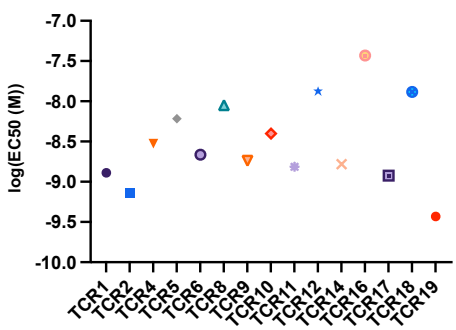

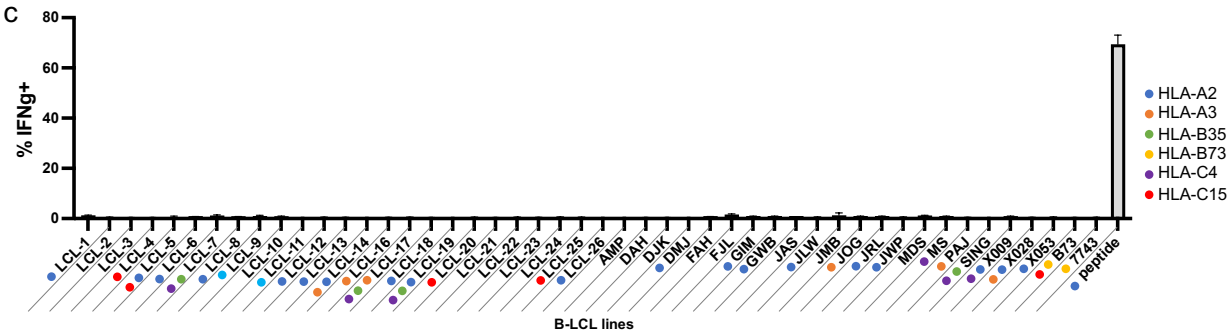

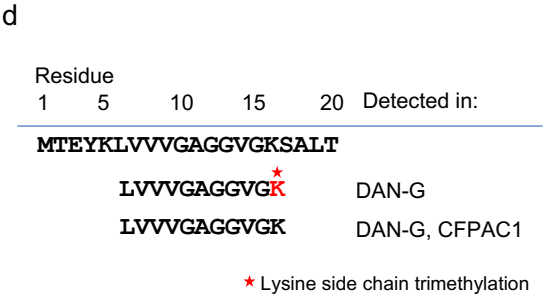

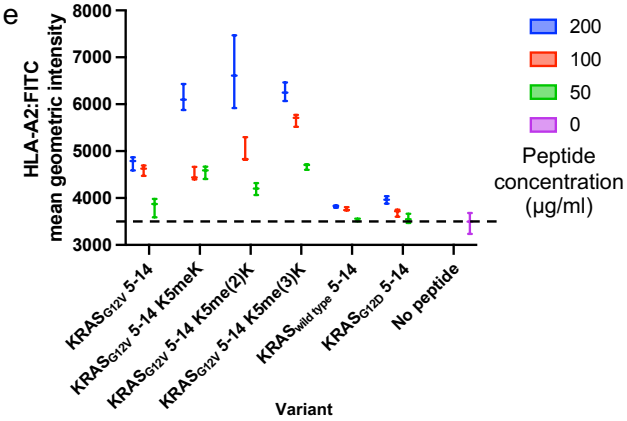

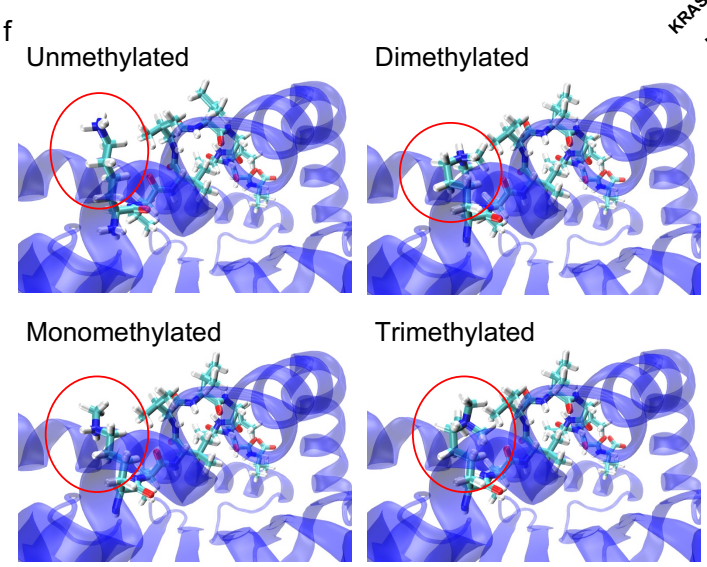

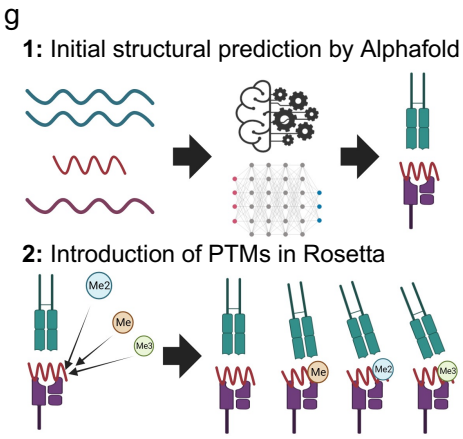

932

933 **Fig. S1:** HLA-A2-presented $KRAS_{G12V}$ epitope includes a lysine residue that can be stably presented with

934 potential side chain methylation. (a) NetMHCPan 4.1 summary of the top 10 peptide sequences that are
935 most likely to be presented by HLA-A2 from the first 30 amino acids of $KRAS_{G12V}$. Peptides containing
936 the G12V mutation (including mutations in red text) are in black text; others are in gray. (b) $Log_{10}(EC_{50}$
937 (M)) comparison of recognition of synthetic $KRAS_{G12V}$ 5-14 peptide (KLVVVGAVGV) presented by
938 HLA-A2 by an initially generated set of MHC class I-restricted TCRs isolated to be specific for this
939 epitope. Lower values indicate higher functional avidity. (c) % $IFN\gamma^+$ T cells, transduced with TCR_2, after
940 exposure to B-LCL cell lines expressing different Class I HLA alleles found on CFPAC1 cells without
941 $KRAS_{G12V}$ 5-14 peptide loaded. Cell lines are color coded by allele. (d) MS results of RAS family peptide
942 fragments detected after tryptic digestion of immunoprecipitated whole KRAS protein from cell lysate of
943 DAN-G and CFPAC1 pancreatic adenocarcinoma cell lines. Lysine side chain trimethylation is indicated
944 in red with an asterisk. (e) Reconstitution of properly folded HLA-A2 surface expression on T2 cells after
945 exogeneous loading by wild type or G12V/D mutant KRAS 5-14 peptides with or without lysine-5 side
946 chain methylations. (f) Additional views of structural models of HLA-A2-presented $KRAS_{G12V}$ 5-14
947 peptide including possible lysine-5 side chain methylation, supplementing Fig. 1e by highlighting the
948 protrusion of the lysine-5 side chain (circled in red) out of the HLA-A2 groove. (g) Overview of structural
949 prediction of a TCR-pMHC complex using a combined Alphafold-Rosetta pipeline. Alphafold allows for
950 deep learning-based prediction of proteins and protein complexes, which we applied to predict TCR-
951 pMHC complex structure. However, this does not yet contain PTMs, which Alphafold cannot incorporate
952 reliably. Thus, we used the resulting structure as input into Rosetta, which used physics-based energy
953 functions to introduce PTMs and reoptimize the structure to accommodate them.
954
955

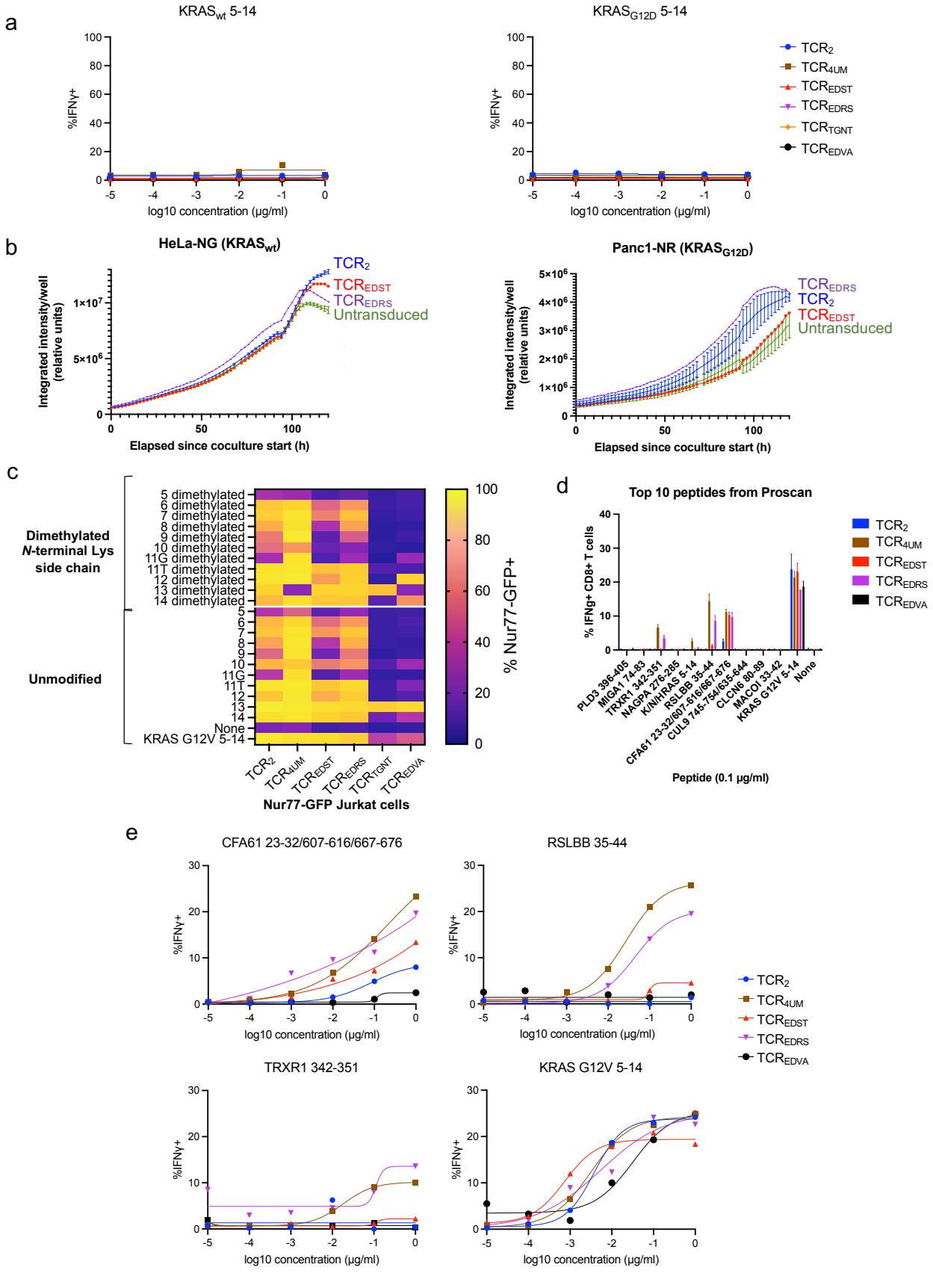
a
KRASwt 5-14
KRASG12D 5-14
%IFNγ+
log10 concentration (μg/ml)
TCR2
TCR4UM
TCREDST
TCREDRS
TCRTGNT
TCREDVA
b
HeLa-NG (KRASwt)
Panc1-NR (KRASG12D)
Integrated intensity/well (relative units)
Elapsed since coculture start (h)
TCR2
TCREDST
TCREDRS
Untransduced
c
Dimethylated N-terminal Lys side chain
Unmodified
5 dimethylated
6 dimethylated
7 dimethylated
8 dimethylated
9 dimethylated
10 dimethylated
11G dimethylated
11T dimethylated
12 dimethylated
13 dimethylated
14 dimethylated
None
KRAS G12V 5-14
% Nur77-GFP+
Nur77-GFP Jurkat cells
d
Top 10 peptides from Proscan
% IFNg+ CD8+ T cells
PLD3 396-405
MICA1 74-83
TRXR1 342-351
NAGPA 276-285
K/NHRAS 5-14
RSLBB 35-44
CFA61 23-32/607-616/667-676
CUL9 745-754/635-644
CLCN6 80-89
MACO1 33-42
KRAS G12V 5-14
None
Peptide (0.1 μg/ml)
e
CFA61 23-32/607-616/667-676
RSLBB 35-44
TRXR1 342-351
KRAS G12V 5-14

956

957 **Fig. S2:** TCRs developed from a mutagenesis library to recognize post-translationally modified epitopes
958 of HLA-A2-presented $KRAS_{G12V}$ are G12V mutation-specific. (a) Dose response curves of $CD8^+$ T cells
959 expressing selected TCRs generated from the HLA-A2 $KRAS_{G12V}$ TCR mutagenesis library after
960 exposure to wild type or G12D KRAS 5-14 peptides presented by HLA-A2. (b) Failure of $CD8^+$ T cell
961 killing and progressive growth of human HLA-$A2^+$ tumor cell lines that express wild type KRAS (HeLa
962 cervical carcinoma cell line; left) or $KRAS_{G12D}$ (Panc1 pancreatic adenocarcinoma; right) and no
963 $KRAS_{G12V}$. Cocultures of T cells and tumor cells were recorded by Incucyte imaging. Tumor cells
964 expressed nuclear fluorescent protein. NR: red fluorescent protein; NG: green fluorescent protein. (c)
965 Alanine scan of $KRAS_{G12V}$ 5-14 epitope tested against TCRs selected from the mutagenesis library. Each
966 cell indicates the resulting expression of Nur77-GFP upon replacement of a $KRAS_{G12V}$ residue with
967 alanine (or in the case of alanine-11, replacement with either glycine or threonine) and with or without
968 lysine-5 side chain dimethylation. (d) IFNγ secretion by $CD8^+$ T cells expressing mutagenized TCRs after
969 exposure to synthetic peptides from the human proteome fitting the K-x-x-V-V-x-A-x-x-x tolerance
970 pattern identified from the alanine scan shown in (c), with a concentration of 0.1 μg/ml for each peptide.
971 (e) Dose response curves of $CD8^+$ T cells expressing mutagenized TCRs after exposure to the potential
972 human off-target peptides demonstrated above to generate the three largest responses at 0.1 μg/ml:
973 $CFA61_{23\text{-}32/607\text{-}616/667\text{-}676}$, $RSLBB_{35\text{-}44}$, and $TRXR1_{342\text{-}351}$, compared to the $KRAS_{G12V}$ epitope.
974

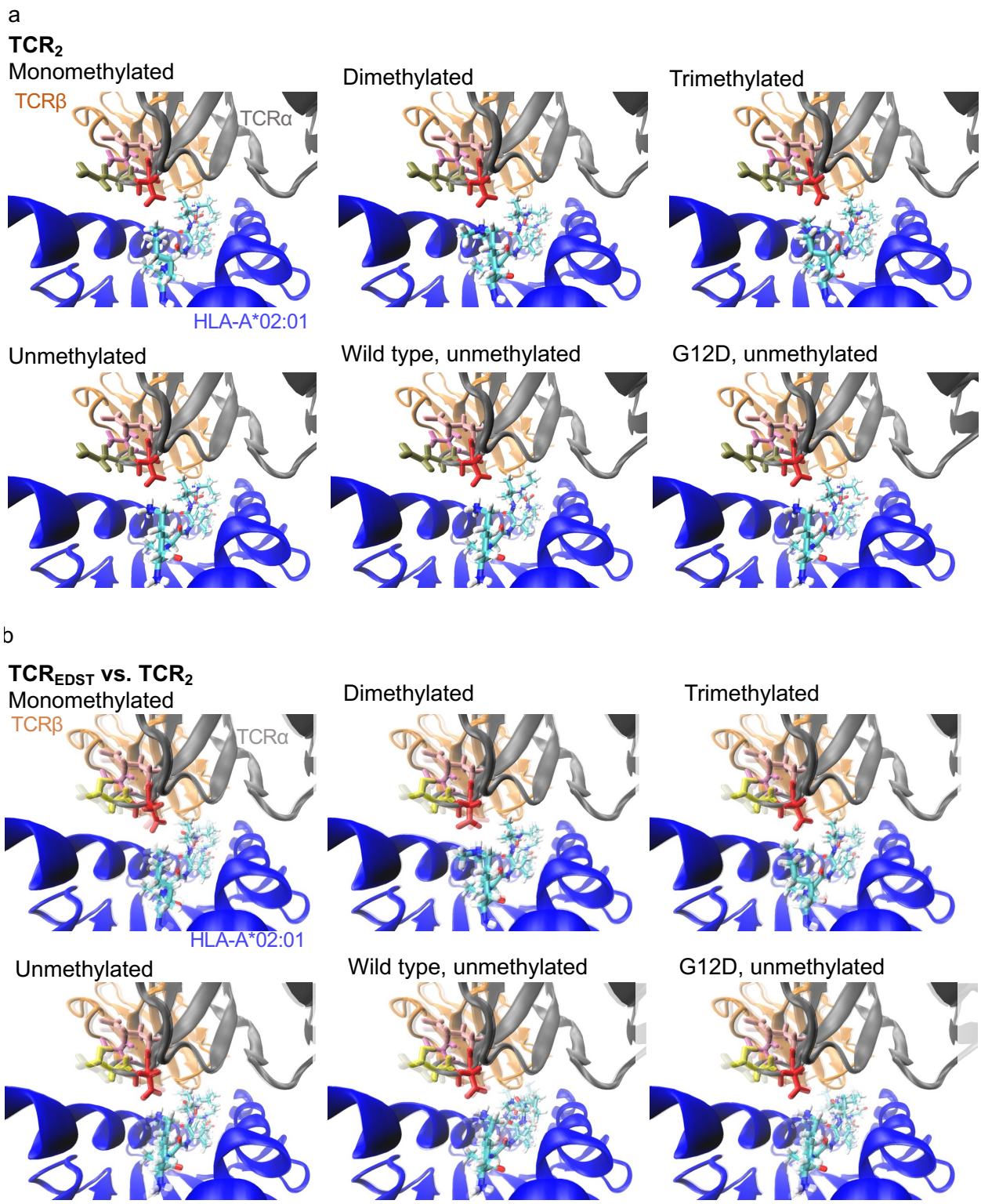

Fig. S3: TCR-pMHC structural models by Alphafold-Rosetta show CDR3α core interactions with N-terminal lysine side chain of HLA-A2-presented $KRAS_{G12V}$ epitope. Structural predictions of

978 unmethylated and methylated variants of $KRAS_{G12V}$ 5-14, as well as unmethylated wild type or G12D
979 peptide, presented by HLA-A2 to interface with (a) TCR_2 and (b) mutagenized TCR_{EDST} TCRs. The
980 CDR3α 'core' sequence is shown as individual amino acids within the TCRs. In (b), the TCR_2-pMHC
981 interfaces from (a) are overlaid with transparency to facilitate visual comparison. With TCR_{EDST}, residues
982 in the core sequence of CDR3α and the lysine-5 side chain of each variant of $KRAS_{G12V}$ epitope appear
983 closer to each other than with TCR_2.

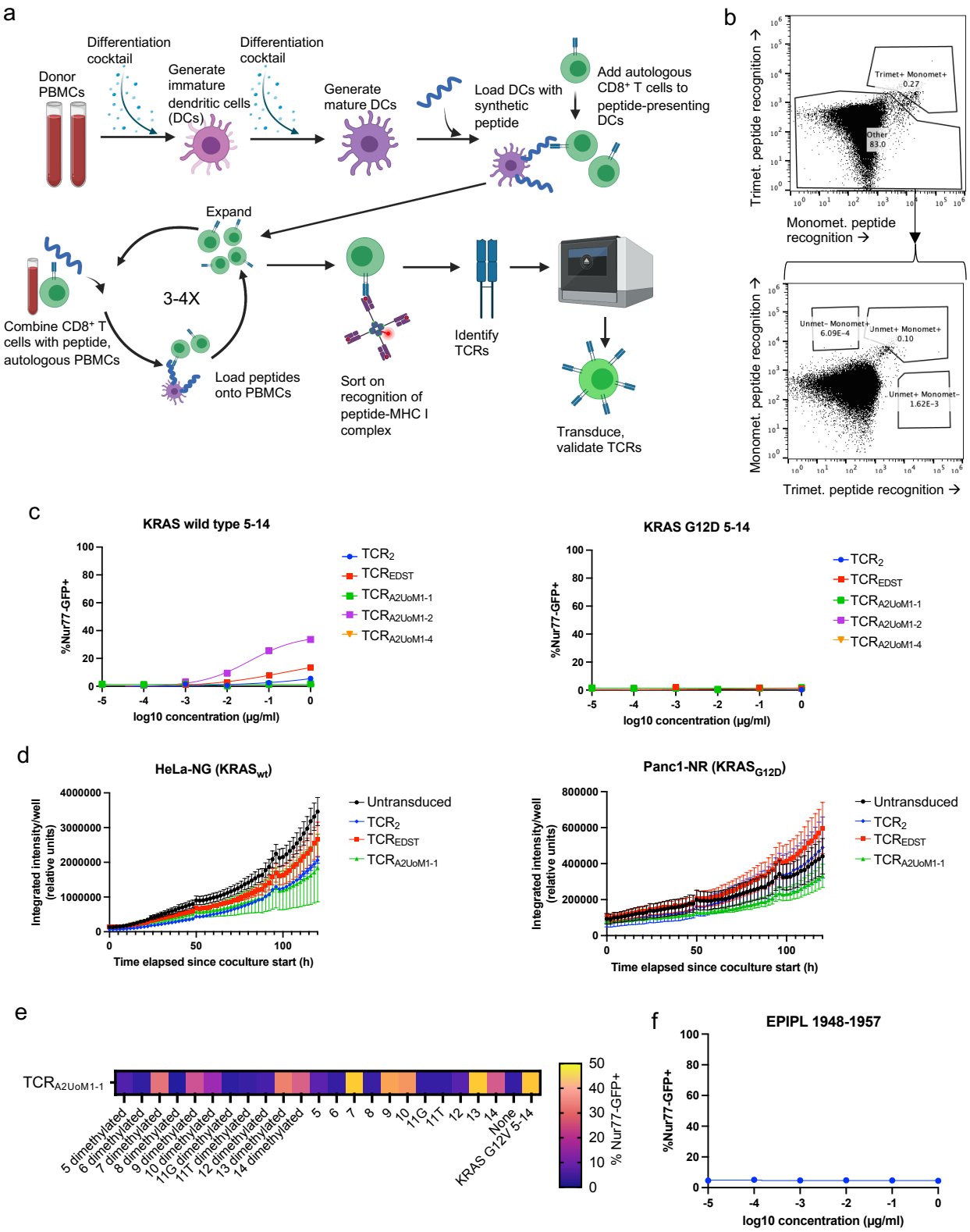

Fig. S4: TCRs identified from primary human T cells specifically target $KRAS_{G12V}$ epitope presented by HLA-A2. (a) Experimental workflow to enrich and characterize T cell clones with TCRs recognizing a

987 defined peptide epitope. (b) Tetramer binding patterns of primary human T cells stimulated with
988 unmethylated and methylated $KRAS_{G12V}$ peptide presented by HLA-A2. Plots also indicate gates used to
989 sort cells with different affinities for unmethylated and methylated epitopes. (c) Dose response curves of
990 TCRs against wild type and $KRAS_{G12D}$ 5-14 peptides presented by HLA-A2. (d) Tumor cell growth
991 during coculture of $CD8^+$ T cells expressing selected TCRs with HLA-$A2^+$, wild type KRAS HeLa and
992 $KRAS_{G12D}$ Panc1 pancreatic adenocarcinoma cell lines. Cocultures of T cells and tumor cells were
993 recorded by Incucyte imaging. Tumor cells expressed nuclear fluorescent protein. NR: red fluorescent
994 protein; NG: green fluorescent protein. (e) Alanine scan of $KRAS_{G12V}$ 5-14 epitope tested against
995 $TCR_{A2UoM1-1}$. Each box indicates the resulting expression of Nur77-GFP upon replacement of a $KRAS_{G12V}$
996 residue with alanine (or in the case of alanine-11, replacement with either glycine or threonine). (f) Dose
997 response curve of $CD8^+$ Nur77-GFP Jurkat cells expressing $TCR_{A2UoM1-1}$ after exposure to $EPIPL_{1948-1957}$,
998 the potential human off-target peptide as determined from alanine scan results.
999

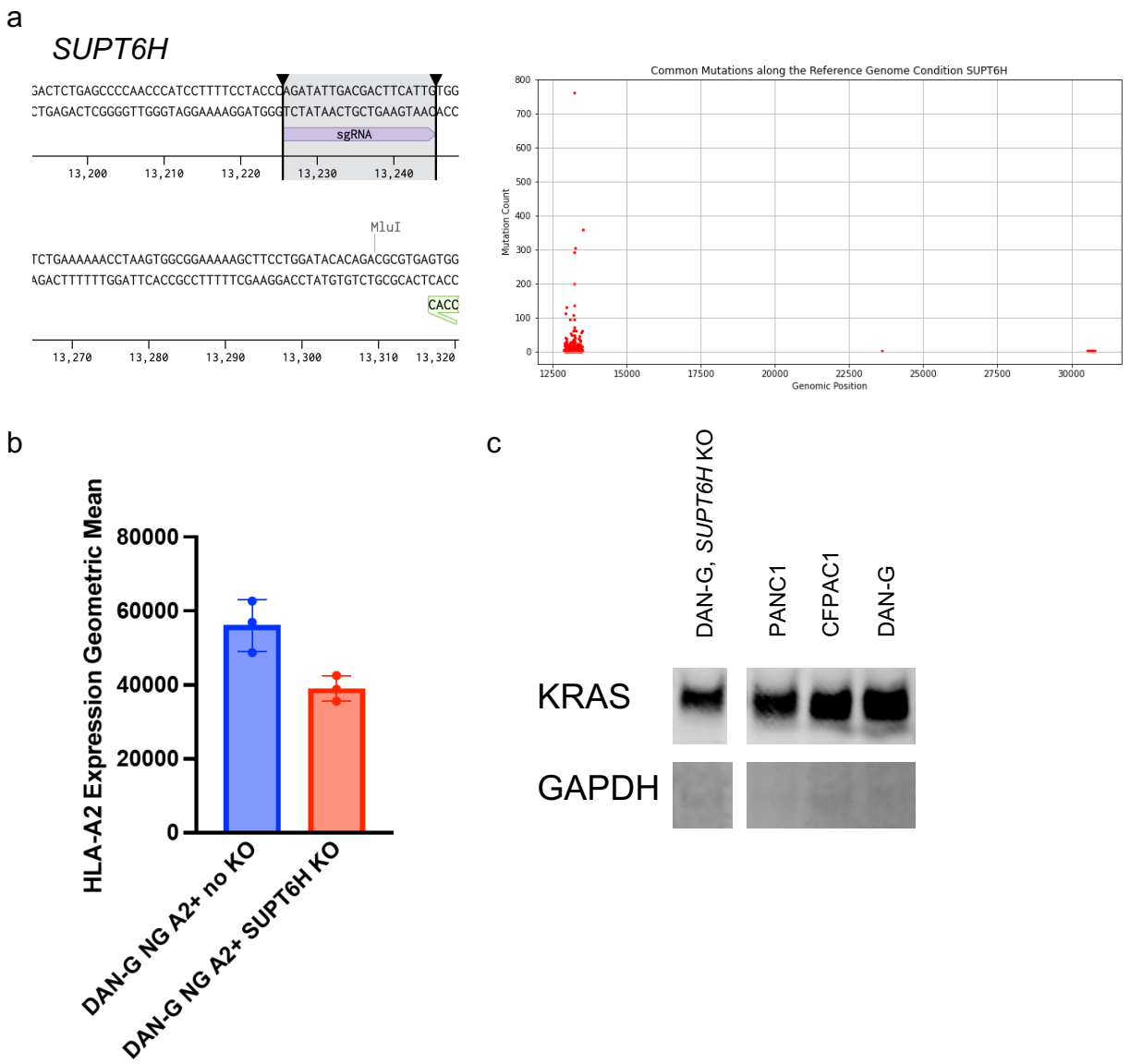

Fig. S5: Further characterization of CRISPR knockout of *SUPT6H*. (a) Location of the gRNA binding region in the *SUPT6H* gene and summary of the genomic position of the commonly occurring mutations detected from DAN-G cells transduced with lentiCRISPRv2 with gRNA targeting *SUPT6H*. Red dots indicate a mutation detected from long-read sequencing. (b) Surface expression of HLA-A2 with and without *SUPT6H* knockout in DAN-G cells. (c) Western blot of total expressed KRAS protein with and without *SUPT6H* knockout in DAN-G cells. KRAS expression in other pancreatic adenocarcinoma cell lines Panc1 and CFPAC1 are shown for additional comparison. GAPDH protein expression was used as a control.

1009 **Table S1:** List of gRNAs for CRISPR knockout screen of methylation-related genes.